Sarcoplasmic Reticulum Calcium Handling in Maturing Skeletal Muscle From Two Models of Dystrophic Mice

By: Matthew R. Rittler

Submitted to the Faculty at Virginia Polytechnic Institute and State University in partial fulfillment of the requirements for the degree of Master of Science in the Department of Human Nutrition Foods & Exercise

Dr. Robert W. Grange – Committee Chair

Dr. Jay H. Williams – Committee Member

Dr. Robert B. Duncan – Committee Member

October 23rd, 2002
Blacksburg, Virginia

Abstract

MATTHEW ROBERT RITTLER
Sarcoplasmic Reticulum Calcium Handling in Maturing Skeletal Muscle From Two Models of Dystrophic Mice.
(Under the direction of Robert W. Grange)

Duchenne's muscular dystrophy (DMD) is a debilitating disease that affects approximately 1 in 3500 boys, with many DMD patients dying before the age of 20 due to cardio-respiratory complications. DMD is the result of defects in the gene that encodes dystrophin, an integral muscle membrane protein. Although the genetic defect has been identified, the relation between the absence of expressed dystrophin and the mechanisms leading to its onset are still unclear. One possibility is that disrupted calcium (Ca^{2+}) handling by the sarcoplasmic reticulum (SR) leads to an increased cytosolic Ca^{2+} concentration that activates proteolytic and apoptotic pathways that initiate muscle fiber death. However, little is known about the role of disrupted SR function in the onset of DMD.

The purpose of this study was to test the hypothesis that altered calcium cycling by the SR could contribute to elevated cytosolic Ca^{2+} levels in the early stages of DMD, and thereby account for the onset of disease pathogenesis. Rates of SR Ca^{2+} uptake and release were determined in quadriceps muscles obtained from maturing dystrophic and control mice prior to the overt signs of the disease at ages ~9 and 21 days. In addition, the content of several key Ca^{2+} handling proteins, including two isoforms of the sarco(endo)plasmic reticulum ATPase pump (SERCA 1 & 2), ryanodine receptor type 1 (RyR1), parvalbumin, and calsequestrin were determined by Western analysis. Two dystrophic mouse models were used, the mdx mouse which lacks dystrophin, and the

mdx:utrophin-deficient (mdx:utrn$^{-/-}$) mouse which also lacks utrophin, a protein homolog of dystrophin.

The rate of SR Ca^{2+} uptake in quadriceps muscles of mdx/utrn$^{-/-}$ mice aged 21 days was 73.1% and 61.3% higher than age-matched control and mdx muscles, respectively ($p < 0.05$). There was no difference in SR Ca^{2+} release rates between the genotypes at either age. There were significant increases in the content of each of the calcium handling proteins with age ($p < 0.05$), but no significant differences were detected between genotypes at either age. These data demonstrate the Ca^{2+} release rates of dystrophic SR are not compromised, but suggest the increased uptake rates of mdx:utrn$^{-/-}$ SR may be an adaptation to increased cytosolic calcium levels, and/or be due to changes in intrinsic SERCA function and/or regulation. The role of increased SR Ca^{2+} uptakes rates in onset of DMD pathogenesis can not be directly determined from the present data; therefore it is suggested that future studies directly assess cytosolic Ca^{2+} concentration and examine the role of SERCA regulatory proteins in intact fibers obtained from mdx:utrn$^{-/-}$ muscles at age 21 days.

Acknowledgements

There are many individuals that I want to thank for getting me to this point in my life. First and foremost, I would like to thank my entire family for their encouragement. They have kept me levelheaded through stressful times and heard me out when I needed to talk. I am so grateful to them.

Secondly, I would like to thank my committee members, Dr. Grange, Dr. Williams, and Dr. Duncan, for their encouragement and advice. They truly helped me do my best on this thesis project and taught me so much.

I would like to thank the other graduate students in the lab. Thank you for making the time in the lab enjoyable. I have to extend a special thanks to Simon Lees, Jeff Otis, and Tommy Gainer for their help in teaching me the laboratory procedures that I needed to know and answering any questions I may have had.

Finally, I would like to thank my girlfriend Ali Arner and all my friends for supporting me, listening to me, and making me laugh when I needed it. I am so thankful for having you all in my life.

Table of Contents

List of Tables

List of Figures

List of important definitions

1. DMD: Duchenne's muscular dystrophy
2. DGC: Dystrophin-glycoprotein complex
3. Ca^{2+}: Calcium
4. $[Ca^{2+}]_i$: Intracellular calcium concentration
5. SR: Sarcoplasmic Reticulum
6. SERCA: Sarco-endoplasmic reticulum calcium ATPase
7. SERCA 1: Type 1 SERCA—referred to as the "fast-type" SERCA, found in muscles of a predominately fast phenotype.
8. SERCA 2: Type 2 SERCA—referred to as the "slow-type" SERCA, found in muscles of a predominately slow phenotype.
9. RyR: Ryanodine receptor
10. RyR1: Type 1 RyR—often defined as the "skeletal-muscle" isoform of RyR, found predominately in, but not limited to, skeletal muscles.
11. PARV: Parvalbumin
12. CSQ: Calsequestrin
13. AU: Arbitrary units

Chapter 1: Introduction

Introduction

Duchenne's muscular dystrophy is the most common and fatal form of all muscular dystrophies, affecting 1 in 3500 boys (Emery, 1993). The disease manifests itself at ~2-3 years of age as initial muscle weakness that progresses to widespread muscle fiber necrosis (Mendell et al., 1991). Ultimately, functioning contractile muscle fibers are replaced with non-contractile fat and connective tissues (Cozzi et al., 2001). The muscle fiber degeneration associated with DMD often leads to the death of patients between their late teens and early twenties due to failure of cardiac and respiratory muscles (Petrof, 1998). The genetic defects associated with DMD are deletions or non-sense mutations in the gene encoding the protein dystrophin (Hoffman et al., 1987; Campbell, 1995; Mendell et al., 1995; Petrof 1998).

The skeletal muscle isoform of dystrophin is a 427-kDa rod-like cytoskeletal protein localized to the inner surface of the sarcolemma. It forms part of the DGC, which links the subsarcolemmal cytoskeleton and the extracellular matrix (Straub and Campbell, 1997). The specific function(s) of dystrophin and the DGC are not yet known, although it is widely believed that they serve both mechanical and signaling roles (Roberts, 2001). It is clear however, that in the absence of this integral protein, death of children affected with DMD will continue to be inevitable until the mechanism(s) is (are) clearly defined and appropriate therapeutic interventions are developed.

Statement of Problem

There are three key hypotheses to explain the onset of DMD: (1) mechanical disruption, (2) signaling disruption, and a subset of the signaling hypothesis, (3) Ca^{2+} dysregulation. At present, none of these hypotheses can fully explain the onset of this deadly disease. It is not known if the mechanism or mechanisms represented by each is solely responsible, or if they all contribute to the pathogenesis at different stages of the disease, or if and when they work in concert. Few studies have addressed these hypotheses prior to the onset of the disease. This study, therefore, focused on one aspect of the Ca^{2+} dysregulation hypothesis: potential disruptions in the cellular mechanisms of Ca^{2+} handling in mouse models of DMD prior to the overt signs of the dystrophic process.

Mechanical. The mechanical hypothesis suggests that when dystrophin is absent, the muscle membrane is not stable, can be readily damaged during contraction and will eventually lead to widespread muscle degeneration. Although reasonable, this hypothesis is predominantly based on studies conducted in older dystrophic mice following the onset of the disease process (e.g., Petrof et al., 1993). In addition, a recent study that examined skeletal muscles of young dystrophic mice prior to the overt signs of the disease demonstrated minimal membrane damage following a contractile challenge *in vitro* (Grange et al., 2002).

Signaling. The signaling hypothesis suggests that, in the absence of dystrophin and the associated proteins of the DGC, one or more signaling pathways essential to normal cellular function are disrupted. For example, recent

observations in dystrophic mice have suggested that when dystrophin is absent, gene expression of several key proteins involved in gene transcription are down regulated (Tkatchenko et al., 2000). At present, this hypothesis is not well-defined as there are a host of potential signaling pathways that could alone or in concert with others, lead to the onset of DMD (e.g., a nitric oxide mediated pathway; Wehling et al., 2001). At present, an approach that assesses the up-regulation or down regulation of a wide range of genes simultaneously (e.g., gene expression analysis using a commercially available gene chip) may be the most efficient to test the signaling hypothesis (e.g., Tkatchenko et al., 2000).

Calcium. Because Ca^{2+} is a critical 2nd messenger in many cell processes (Berchtold et al., 2000), the Ca^{2+} hypothesis can be considered a subset of the signaling hypothesis. This hypothesis states that $[Ca^{2+}]_i$ levels are elevated in dystrophic muscle fibers because dystrophin and the DGC are absent from the muscle sarcolemma. This deficiency then leads to disrupted cellular processes such as increased Ca^{2+}-dependent proteolytic activity. However, it is critical to understand that the link between dystrophin and alterations in $[Ca^{2+}]_i$ has not yet been clearly established. Most notably, there is considerable controversy about whether Ca^{2+} levels are altered in dystrophic muscle (Gillis et al., 1996). Certainly, if chronically higher levels of Ca^{2+} did occur then activation of Ca^{2+}-dependent proteases would represent a very reasonable mechanism to initiate DMD (Tidball & Spencer, 2000). However, although there is reasonable evidence in the literature to describe how Ca^{2+} homeostasis may be altered after the onset of the dystrophic process, it is still not known if Ca^{2+} homeostasis may

be altered before the onset of the dystrophic process. Further, it is not presently known if such disruptions in Ca^{2+} homeostasis could then also account for the onset of DMD.

Alterations in Ca^{2+} homeostasis could result from leaky sarcolemma membranes in the absence of dystrophin and the DGC, and/or from problems in the primary calcium handling organelle in muscle fibers, the SR. Altered SR function could result from disruptions in, as yet, unidentified signaling pathways that might impact gene expression of proteins involved in Ca^{2+} handling such as RyR, the SERCA, or a calcium binding protein such as PARV. This study focused on SR function. The purpose of this study, was to determine if Ca^{2+}-handling mechanisms associated with the SR are altered in mouse dystrophic models of DMD in a manner consistent with increased $[Ca^{2+}]_i$. For example, increased Ca^{2+} release from the SR per activating pulse coupled with slowed uptake of Ca^{2+} into the SR could lead to elevated cytosolic Ca^{2+} concentrations, and thereby contribute to the onset of the dystrophic phenotype.

Significance of Study

DMD is a severe debilitating and fatal disease. The mechanism(s) of onset are presently unclear as there have been few studies conducted prior to the overt signs of the disease, even in dystrophic animals models such as mice (e.g., the early maturation period prior to weaning). A strong candidate hypothesis is that disrupted Ca^{2+} handling in the dystrophic muscle cells leads to an increased cytosolic Ca^{2+} concentration. Myoplasmic Ca^{2+} concentrations are regulated

primarily by the uptake and release mechanisms of the SR. Thus, it is logical to assess these biochemical functions as well as the protein content of some of the key proteins involved, to determine if Ca^{2+} handling is disrupted in DMD cells. For example, if Ca^{2+} uptake were slowed in dystrophic muscle, an elevated $[Ca^{2+}]_i$ concentration could result. An increased $[Ca^{2+}]_i$ in dystrophin-deficient cells could induce the activity of Ca^{2+}-activated proteases (i.e., calpains) and result in widespread proteolysis (Badalamente et al., 2000). Alternatively, or together with this proteolysis, the increased Ca^{2+} could trigger a series of apoptotic signals within the mitochondria (Bernardi, 1999). Both of these possibilities could contribute to the initiation of DMD.

Based on this rationale, this study compared Ca^{2+} handling in skeletal muscles obtained from two dystrophic models, mdx and mdx:utrn$^{-/-}$ mice, with that of control mice during early maturation (i.e., prior to weaning) to determine if disrupted Ca^{2+} handling was responsible for or contributed to the onset of DMD.

The goal of this study, therefore, was to delineate the role of Ca^{2+} handling in the onset of DMD, so that the mechanism(s) of onset could be more clearly defined. A clear definition of the mechanism might then lead to development of suitable therapeutic interventions.

Specific Aims

1. To test the hypothesis that calcium cycling (i.e., uptake and release rates) by the SR is compromised in dystrophic muscles during early maturation (e.g., equal to or less than age 21 days), accounting for the onset of the disease.
2. To test the hypothesis that the content of several key Ca^{2+} handling proteins is altered and contribute to disrupted calcium cycling in dystrophin-deficient muscle fibers.

Research Hypotheses

The following are the null hypotheses tested in this study:

H_{01}: There will be no effect of age, genotype, or their interaction on Ca^{2+} uptake rates in the dystrophic mdx and mdx/utrn$^{-/-}$ mice from age-matched control mice during early maturation.

H_{02}: There will be no effect of age, genotype, or their interaction on Ca^{2+} release rates in the dystrophic mdx and mdx/utrn$^{-/-}$ mice from age-matched control mice during early maturation.

H_{03}: There will be no effect of age, genotype, or their interaction on total SERCA content in the dystrophic mdx and mdx/utrn$^{-/-}$ mice from age-matched control mice during early maturation.

H_{04}: There will be no effect of age, genotype, or their interaction on SERCA 1 content in the dystrophic mdx and mdx/utrn$^{-/-}$ mice from age-matched control mice during early maturation.

H_{05}: There will be no effect of age, genotype, or their interaction on SERCA2 content in the dystrophic mdx and mdx/utrn$^{-/-}$ mice from age-matched control mice during early maturation.

H_{06}: There will be no effect of age, genotype, or their interaction on CSQ content in the dystrophic mdx and mdx/utrn$^{-/-}$ mice from age-matched control mice during early maturation.

H_{07}: There will be no effect of age, genotype, or their interaction on PARV content in the dystrophic mdx and mdx/utrn$^{-/-}$ mice from age-matched control mice during early maturation.

H_{08}: There will be no effect of age, genotype, or their interaction on RyR1 content in the dystrophic mdx and mdx/utrn$^{-/-}$ mice from age-matched control mice during early maturation.

Basic Assumptions

The following were the basic assumptions made by the investigator:

1. The mice were well fed and hydrated.
2. Control animals were free from disease.
3. The skeletal muscles of mdx and mdx:utrn$^{-/-}$ mice were suitable models for the study of Duchenne's muscular dystrophy.
4. The SR homogenate fractions retained the capacity to take up and release Ca^{2+}.
5. The antibodies used to detect a given protein were specific; the band intensities on Western blots determined by densitometry reflected the

content of the protein in each sample; and, the protein content could be normalized to the intensity of a control band on the same blot.

Limitations

The following were limitations of the current study:

1. The current study was limited to the quadriceps muscle groups of mice.
2. Due to limited technical capabilities, this project addressed only one aspect of calcium handling in dystrophic muscle (i.e., SR calcium uptake and release rates). The activities of calcium leak channels were not investigated; therefore, the contribution to increased intracellular calcium from these sources was not taken into account.

Chapter 2: Review of Literature

Introduction. Duchenne's muscular dystrophy is a debilitating and fatal disease that affects 1 in 3500 boys (Emery, 1993). The progressive muscle-wasting characteristic of this disease usually claims the life of those affected before the age of 20 years due to failure of cardiac and respiratory muscles (Hoffman et al., 1987). Despite extensive research, the pathogenesis of this disease remains largely unknown, and therefore it is not currently understood what mechanism or mechanisms are responsible for its onset. Although there are several hypotheses, controversy surrounds each as noted below.

Dystrophin and associated proteins. The dystrophin gene is located on the short arm of chromosome X at locus p21, and contains at least 5 promoters. The promoters regulate the expression of three isoforms of dystrophin that are distinctly localized to specific tissues (Campbell, 1995). Because of its large size, there is a greater chance for mutation within the gene, and this may account for the high occurrence of DMD (Petrof, 1998). The skeletal muscle isoform of dystrophin is a 427-kDa rod-like cytoskeletal protein localized on the inner surface of the sarcolemma. It forms part of the DGC, which links the subsarcolemmal cytoskeleton and the extracellular matrix (Straub and Campbell, 1997). The DGC (Figure 1) is composed of dystrophin, α-, β-, γ-, and δ-sarcoglycans (SG), α- and β-dystroglycans (DG), sarcospan (SSPN), dystrobrevin (DB), neuronal nitric oxide synthase (nNOS), and α- & β-syntrophins (Straub and Campbell, 1997; Allamand and Campbell, 2000). Beta dystroglycan,

which interact directly with dystrophin, spans the cell membrane and interacts with α-dystroglycan, which binds agrin and laminin in the extracellular matrix.

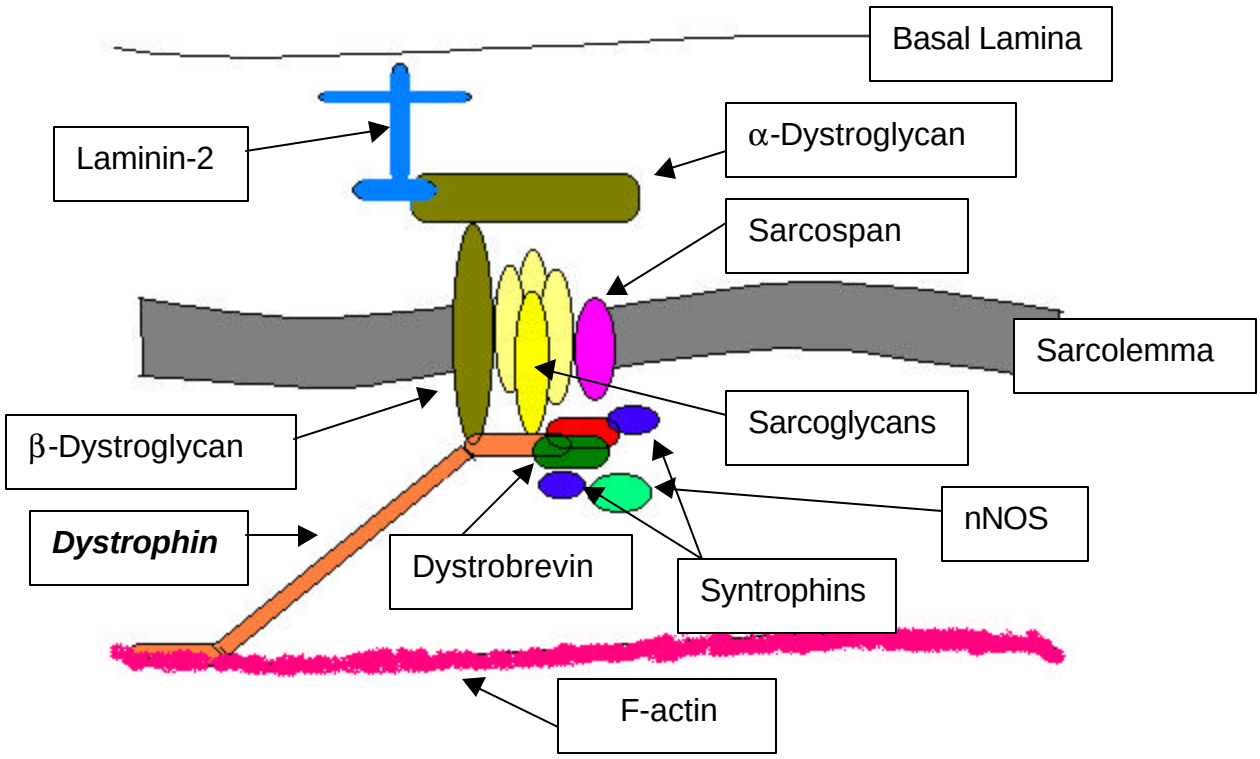

Figure 1: Diagram of the Dystrophin-Glycoprotein Complex (adapted from Roberts, 2001).

Functions of dystrophin and the DGC. The specific functions of dystrophin are not yet fully known, although it is widely believed that it serves both mechanical and signaling roles (Roberts, 2001). Some models suggest that dystrophin mechanically links the intracellular cytoskeleton (F-actin) and the extracellular matrix (laminin) (See Fig. 1). Associations between dystrophin and other proteins associated with the DGC suggest a signaling role (i.e., agrin,

neuronal nitric oxide synthase, voltage gated Na^+ channels, and sarcoglycans) (Roberts, 2001). When dystrophin is absent, the entire DGC is absent from the sarcolemma (Straub and Campbell, 1997); therefore, the potential mechanical and signaling functions of the complex could be compromised. Disruptions in one or both of these functions could lead to onset of DMD.

Animal models of DMD. Because of ethical considerations with tissue samples from DMD patients, investigators have relied heavily on animal models to study the disease (i.e., mouse, canine, cat, etc.). For example, canine X-linked muscular dystrophy (CXMD), best characterized in the golden retriever, is a model very similar to DMD. CXMD is genetically homologous to DMD and the clinical manifestations mimic those seen in the human condition. There is connective tissue proliferation, fiber regeneration, and widespread fiber necrosis, and similar to human DMD, early death (Cozzi et al., 2001). Despite the close similarities, long gestation periods and small litter numbers with this model limits studies requiring large sample numbers.

The mdx mouse is the most commonly used model for DMD. This naturally occurring model has been available for ~17 years (Bulfield et al., 1984). These mice have a point mutation in the 5' end of the dystrophin gene that causes a premature transcriptional stop and results in a truncated protein product. Mdx mice, therefore, are completely devoid of full-length dystrophin in their muscle cells (Sinckinski et al., 1989). Based on the close genetic similarity with DMD patients, the mdx model should be considered ideal, but there are sufficient differences to limit its usefulness. Histological examination of muscles

from these animals between 3-4 weeks of age reveals massive degeneration. However, unlike DMD patients, the degeneration does not continue, as the muscles start to show signs of regeneration after 5 weeks of age (Carnwath and Shotton, 1987). From this point there are cycles of degeneration and regeneration occurring in mdx muscle until approximately 10-11 weeks, when muscle fiber degeneration stops and is delayed until approximately 18 months of age (Stedman et al., 1991). Even when the mice start to again show signs of muscle degeneration, it appears to be localized to a specific muscle: the regenerative capacity of the diaphragm fails and the fibers are gradually replaced by fibrotic tissue and fat. These changes are very different from human DMD, where gradual muscle degeneration of all skeletal muscle continues from onset at an age of ~2-3 years to 20 years. There are other differences, as the muscles of mdx mice do not appear to be significantly weaker than control muscles during early maturation (Grange et al., 2002). These mice are virtually devoid of any clinical features of the disease like stunted growth, labored breathing and early death, as they live a relatively normal lifespan (~2-2.5 years) (Rafael and Brown, 2000; Allamand and Campbell, 2000).

The blunted dystrophic phenotype in mdx muscle may be due to the presence of a closely related protein, utrophin, localized to the muscle fiber sarcolemma. Utrophin is similar to dystrophin in both its primary sequence and predicted secondary structure (Love et al., 1993). It is normally localized to the subsynaptic membrane at the neuromuscular junction and myotendinous junction of adult mammalian skeletal muscle (Rafael et al., 2000). Despite its normal

localization in skeletal muscle, utrophin is readily detectable in extrasynaptic portions of the muscle sarcolemma of regenerating DMD and mdx fibers (Grady et al., 1997). Because of the similarities in the two proteins, it has been suggested that utrophin may “compensate” for any loss of dystrophin in the mouse skeletal muscle membrane in such a way that it attenuates the dystrophic muscle phenotype. Tinsley et al. (1998) demonstrated this potential compensation by expressing full-length utrophin in mdx mouse muscles. Using the human skeletal α-actin (HAS) promoter, transgenic mice expressing full-length utrophin protein in skeletal muscle were produced. The generated mice lines were then crossed with existing mdx strains to produce mice that lacked dystrophin, but expressed utrophin that was localized throughout the sarcolemma of the muscle fibers. Muscle morphology, regeneration, force development, and stretch resistance were assessed in mdx and transgenic mdx muscle fibers from mice aged 10-12 weeks. The results demonstrated that full-length utrophin, when localized to the sarcolemma, caused a complete recovery of normal mechanical function and prevented dystrophic events from forming in the muscle when dystrophin was absent. It was noted that any prevention of fiber necrosis depended directly on the amount of full-length utrophin available in the sarcolemma (Tinsley et al., 1998).

To better understand the structural role of utrophin, a utrophin-null mutant mouse was generated, but these mice only demonstrated minor differences in phenotype compared with normal mice (Grady et al., 1997a). Therefore, to address the potential protective role of utrophin in DMD, a double mutant lacking

both dystrophin and utrophin (mdx:utrn$^{-/-}$) was generated (Grady et al., 1997; Deconinck et al., 1997). The resulting phenotype was more similar to that of human DMD patients than was the phenotype of the mdx mice (Grady et al., 1997). The mdx:utrn$^{-/-}$ mice were similar to wild-type mice at birth, but by age 14 days demonstrated onset of the dystrophic phenotype. Movement was characterized by a waddling gait, due to stiff hind limbs. These mice also demonstrated kyphosis, or curvature of the spine, another common feature of DMD. The severity of these symptoms progressed with age, with only half of the generated mice living past 8 weeks of age (Deconinck et al., 1997). Fiber degeneration, and the subsequent necrosis, was observed earlier and persisted much later than that observed in the muscles of mdx mice. Similar to patients with DMD, death of the mdx:utrn$^{-/-}$ mice was premature and was the direct result of fatal wasting of skeletal and cardiac muscle (Grady et al., 1997). Because the mdx:utrn$^{-/-}$ mice demonstrated pathological characteristics more consistent with DMD, they appeared to be a suitable model to provide insights into the pathogenesis of and possible therapeutic strategies for DMD (Grady et al., 1997; Deconinck et al., 1997).

Although the pathological similarities between mdx mice and young boys with DMD are questionable, at present, they remain a widely used genetic mouse model of the disease. Utrophin expression is increased in DMD patients, but any attenuation of the disease process appears to be minor (Deconinck et al., 1997). Because the mdx mouse is genetically similar to the human condition, it may still provide important information about human DMD and the use of these mice

should continue. The mdx/utrn$^{-/-}$ model may also prove beneficial to the study of DMD, as these mice have phenotypic symptoms that more closely resemble those observed in the human condition. Both dystrophin mouse models, if used at an age after the onset of dystrophy, can be used to study the changes that occur in muscle during the dystrophic process. However, if these mice are studied at young ages (i.e., before the onset of dystrophy) they could provide insight into how the disease process is initiated—an answer that still eludes investigators.

Dystrophin deficiency—The mechanical hypothesis. The link between the loss of dystrophin and the associated proteins of the DGC and the onset of DMD is not clearly defined. Several hypotheses describe possible biological roles for dystrophin and the DGC in the normal muscle cell that may impact the dystrophic muscle cell in their absence. The mechanical hypothesis suggests that dystrophin and the DGC act to mechanically stabilize the sarcolemma. The DGC, along with additional proteins located near the sarcolemma, form lattice-like structures on the cytoplasmic side of the plasma membrane known as costameres (Campbell, 1995). Costameres act to distribute forces generated in the sarcomere during contraction (Danowski et al., 1992). Although dystrophin comprises only 0.002% of total muscle protein and 5% of total membrane protein content (Hoffman et al., 1987), it is believed to provide substantial structural stability to the muscle sarcolemma. In the absence of dystrophin, the proteins of the DGC are dispersed within the cytoplasm. It is believed that complete loss of the DGC weakens the muscle plasma membrane (Ibraghimov-Bestrovnaya et al.,

1992). In DMD, it is commonly believed that the already weakened membrane continues degrading as the disease progresses (Mendell et al., 1995). Furthermore, it has been hypothesized that contraction of dystrophic muscle leads to even more damage, worsening the disease state (Petrof et al., 1993).

In a study investigating the possible function of dystrophin in the muscle fiber sarcolemma, Pasternak et al. (1995) directly measured the stress-strain relationship of fiber membranes. The investigators hypothesized that if dystrophin provided mechanical stability to the sarcolemma, muscle cells without dystrophin compared to cells with dystrophin should be less stiff. In this study, myotubes cultured from primary satellite cells of normal and mdx skeletal muscle were used. Deformability of the fiber sarcolemma was measured as the resistance to indentation of a small area of the cell surface by a glass probe 1 μm in radius. Stiffness is the ratio of the change in force for a given change in length; therefore, in this study, stiffness was determined from the increment of force (mdyne) per μm of indentation. Normal myotubes, on average, were fourfold stiffer than myotubes cultured from mdx mice, indicating a substantial reduction in stiffness of cells lacking dystrophin. These results suggested dystrophin and its associated proteins provided some reinforcement to the muscle cell membrane.

Petrof et al. (1993) demonstrated that muscles from older mdx compared to control mice were more susceptible to contraction-induced sarcolemmal rupture. In this study, isolated diaphragm strips and EDL muscles from 90- to 110-day-old control and mdx mice were subjected to various muscle contraction

protocols. The eccentric contraction protocol consisted of 5 periods of electrical stimulation at a frequency of 80 Hz for 700-ms. Over the final 200-ms of stimulation muscles were stretched at a velocity of 0.5 of the optimal length of the muscle (L_0; length at which isometric twitch response is maximal)) per sec through a distance that was 0.1 L_o. The isometric protocol consisted of 5 periods of stimulation for the same duration as for the eccentric contraction protocol, with the muscle maintained at L_o. In the passive stretch protocol, muscles were stretched as described for the eccentric protocol but without stimulation. For each of these protocols, muscles were allowed to recover for 4 minutes between each stimulation or stretch (with muscle length maintained at L_0). A final protocol consisted of repeated submaximal isometric stimulations (approximately 450 contractions) at a frequency of 30 Hz over a 5-minute period. During all protocols, the muscles were incubated in oxygenated 0.2% procion orange/Ringer's solution. Procion orange is a fluorescent dye used to detect sarcolemmal damage because of its small molecular weight (M_r 631). Intact muscle cells are impermeable to the dye; therefore, damaged membranes could be easily distinguished in transverse muscle sections by the presence of dye within the fiber. After the eccentric contraction protocol there was approximately a 3% and 16% increase in the percentage of dye-positive fibers in control and mdx EDL muscles, respectively. However, Petrof et al. (1993) reported a weak linear relationship ($r \sim 0.60$) between the force loss exhibited by the mdx muscles and the proportion of fibers that showed damage. The number of muscle activations (e.g., isometric) was not correlated to the extent of damage. These

results implied that a possible function of dystrophin was to provide mechanical reinforcement to the muscle membrane to protect it from stresses imposed during high-force eccentric muscle contractions (Petrof et al. 1993).

In a recent study by Lynch et al. (2000), the contraction-induced injury hypothesis was tested in 6-month-old control, mdx, and transgenic mdx (tg-mdx) mice. The purpose of the investigation was to assess force deficits in the dystrophin-deficient muscles, and to determine if the deficits were the result of a damaged contractile apparatus or other factors within the myofiber itself. The tg-mdx mice over-expressed dystrophin and showed no morphological or functional signs of dystrophy. Extensor digitorum longus (EDL) muscles from 6-month-old male mice of all genotypes were chemically skinned to disrupt the sarcolemma of the muscle fibers. The absence of the sarcolemma in these experiments eliminated any protection conferred from dystrophin or the DGC. After permeabilization, the fibers were maximally activated with calcium and then stretched to 10%, 20%, and 30% of their optimal length. The magnitude of injury was assessed immediately following the strain protocol by measuring the deficit of force generated in the muscles before and after stretch. There was always less force generated after stretch; therefore, the force deficit was expressed as a percentage of the initial force generated. No significant differences were observed in force deficits among the different strains. Lynch et al. (2000) showed that in the absence of the sarcolemma, no differences in injury-susceptibility were observed for dystrophic muscle compared to control muscle. Brooks (1998) observed that in whole EDL muscles from mdx mice of similar age

(~6 months) but not subjected to chemical skinning, there was a 20% greater force deficit compared to those of control mice. These results implied the force loss was due to membrane damage. Considered collectively, the results of Lynch et al. (2000) (absence of the sarcolemma) and the results of Brooks (1998) and others (presence of sarcolemma) indicate the dystrophic force deficits do not arise from a disrupted contractile apparatus, but rather from disruptions in the sarcolemma. Lynch et al. (2000) suggested that an intact sarcolemma could provide significant protection from injury during fast, powerful contractions.

This mechanical hypothesis is often used to explain how DMD is initiated, but this is based primarily on muscle responses obtained from older dystrophic mice well beyond the onset of the disease. For example, signs of muscle degradation in the mdx mouse become apparent in hindlimb skeletal muscle at 3-4 weeks of age and in the mdx:utrn$^{-/-}$ mice at 2-3 weeks (Deconinck et al., 1998; McGeachie and Grounds, 1999), and for both, the degradation continues until at least age 10 weeks. However, the age of the mice used in many of the mechanical studies were 10 weeks and older (e.g., Petrof et al., 1993, Pasternak et al. 1995, Deconinck et al., 1998, Lynch et al., 2000). In a recent study by Grange et al. (2002) the role of mechanical injury in the initiation of DMD was assessed in EDL muscles from maturing control, mdx, and mdx/utrn$^{-/-}$ pups. EDL muscles from 9-12 day-old pups were subjected to a stretch-injury protocol similar to that used by Petrof et al. (1993). Young mdx and mdx:utrn$^{-/-}$ muscles demonstrated modestly greater membrane damage (~7-9%) compared to control (~3%) in both the stretched and unstretched conditions. Surprisingly, neither of

the dystrophic models demonstrated greater membrane damage in the stretched (~7-8%) vs. unstretched (~7-8%) conditions (Grange et al., 2002). These results are of particular interest when considering the initiation of the dystrophic process, because they suggest that maturing dystrophic muscles do not appear to be susceptible to membrane damage during acute mechanical stress. These data strongly suggest that contraction- and stretch-induced membrane damage may not be the cause for the onset of the dystrophic phenotype, and that instead signaling may play a prominent role. When the results of the above studies are considered collectively, the mechanical hypothesis does not appear to adequately explain the initiation of DMD.

Dystrophin deficiency—The signaling hypothesis. The signaling hypothesis suggests that dystrophin interacts with membrane proteins to provide signal transduction between the cytosol and the extracellular matrix (Tidball and Law, 1991), and in its absence, one or more signaling functions are lost. For example, dystrophin through the DGC could interact with integrins, a family of proteins that are critical to transmembrane signaling (Burkin, et al., 2001). Similarly, neuronal nitric oxide synthase (nNOS) is associated with the syntrophins of the DGC. This protein is thought to help regulate functional hyperemia by signaling relaxation of vascular smooth muscle through an NO-cGMP-mediated pathway (Lau et al., 2000; Grange et al., 2001). When dystrophin is lost, nNOS content at the sarcolemma is also decreased (Chang et al., 1996). Interruption of this signaling pathway could lead to ischemia (Chang et al., 1996; Lau et al., 2000; Grange et al., 2001). At present the signaling

hypothesis is the least well defined, as there are a host of potential signaling pathways that could alone or in concert with others, lead to the onset of DMD. A strong candidate as a signaling molecule involved in DMD, however, is Ca^{2+}, a well-known second messenger in a host of cell signaling pathways (Berchtold et al., 2000). At present, the effect of the absence of dystrophin and the DGC on Ca^{2+} handling has not been well characterized.

Dystrophin deficiency--The calcium hypothesis. Calcium contributes to and controls a large number of biochemical processes within muscle cells. Most importantly, Ca^{2+} acts as an intermediate signaling ion in excitation-contraction-coupling (ECC). In skeletal muscle, ECC does not depend on the entry of external Ca^{2+} (Adams & Beam, 1990). Although L-type Ca^{2+} channels (dihydropyridine receptors) located within the T-tubules of the sarcolemma open slowly and allow the entry of Ca^{2+} into the myoplasm during depolarization (Strube et al., 2000), the main source of $[Ca^{2+}]_i$ for contraction comes from the SR located within the muscle fiber. The cyclical release and uptake of Ca^{2+} from and to the SR, also termed Ca^{2+} cycling, maintains cytosolic $[Ca^{2+}]_i$ and thereby regulates the rhythmical contraction-relaxation processes in skeletal muscle, as well as additional Ca^{2+}-dependent processes within the cell. Thus, the mechanisms associated with Ca^{2+} handling are critical to the viability of muscle cells.

The RyR, located on the SR membrane, is the major channel for Ca^{2+} release from the intracellular pools in skeletal muscle. Fast and slow skeletal muscle fibers contain predominately RyR1, and the density of RyR changes

depending on fiber type (i.e., density is higher in fast fibers) (Berchtold et al., 2000).

To begin the ECC process, a neuronal signal originating in a motor neuron and acting via the neuromuscular junction sends an action potential, or wave of depolarization, over the sarcolemma. The action potential spreads over the plasma membrane of the muscle fiber and moves transversely into the fiber via the T-tubules. Depolarization in the T-tubule initiates the Ca^{2+} release process (Fleischer & Inui, 1989). The dihydropyridine receptors (DHPR) located in the T-tubule membrane serve as voltage sensors for ECC, and for this reason, they are located very close to the Ryr Ca^{2+} release channels of the SR (Adams & Beam, 1990). It is commonly believed that signals are transmitted from DHPR to RyR via "mechanical" coupling (Figure 2) (Felder et al., 2002). RyR are activated by low Ca^{2+} concentrations (i.e., 50% activation at 0.5 μM) and are inhibited at higher Ca^{2+} concentrations (i.e., 50% inhibition at 0.15 mM). This positive and negative feedback leads to a bell-shaped curve representing Ca^{2+} release from the RyR (Berchtold et al., 2000). Therefore, when RyR are activated by T-tubule depolarization, released Ca^{2+} results in a further increase in the rate of Ca^{2+} release, and this is soon followed by a reduction in Ca^{2+} release rate as myoplasmic Ca^{2+} concentrations rise (Berchtold et al., 2000). The reason for this feedback control is to regulate the cytosolic Ca^{2+} levels within the muscle fiber, both to provide control for contraction, as well as to avoid activation of processes detrimental to the cell such as Ca^{2+} - dependent proteolytic pathways.

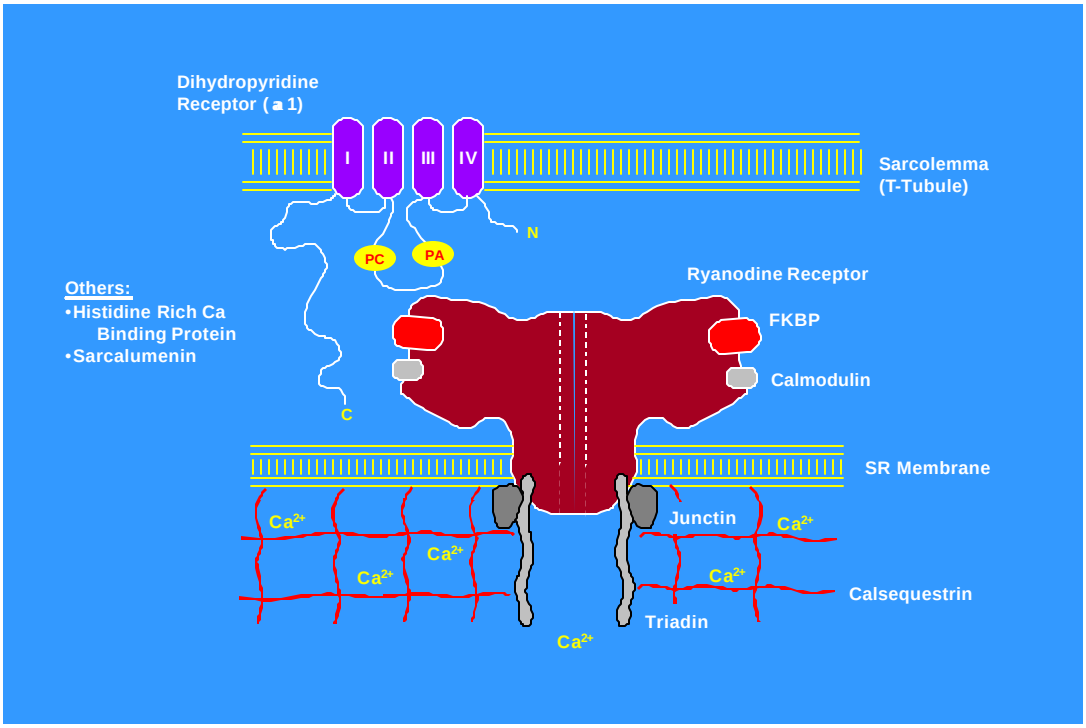

Figure 2: Diagram of the interaction of t-tubules and the SR and proteins involved in ECC.

After release from the SR, Ca^{2+} binds to one of the troponin subunits (TnC) that forms a regulatory complex with tropomyosin on the thin filament of the contractile apparatus. The binding of Ca^{2+} to the troponin-tropomyosin complex reveals the myosin-binding sites on actin so that myosin heads can then bind to the actin filament. When myosin heads bind to the actin filament (cross-bridge formation), ATP is hydrolyzed by the myosin ATPase activity within the myosin heads to provide the necessary energy for the thick myosin filament to pull on the thin actin filament. Therefore, binding of Ca^{2+} to the myofibrillar switch protein, Troponin C is followed by the development of tension and eventual

muscle contraction (Berchtold et al., 2000; Moss, 1992). The action of millions of cross-bridges in many muscle fibers allows the muscle to shorten.

After contraction, several events occur to facilitate muscle relaxation. (1) Calcium dissociates from TnC. (2) Calcium must translocate to the SR, so that (3) uptake into the SR by SERCA can occur. A protein that is of particular importance in fast-type muscle fiber relaxation is PARV (Figure 3). Positive correlations between PARV content and relaxation rates observed in fast-twitch skeletal muscle suggest that PARV facilitates Ca^{2+} translocation to the SR (Berchtold et al., 2000). Parvalbumin levels are found in high concentrations in skeletal muscle fibers of the fast phenotype (Berchtold, 1989). After Ca^{2+} has translocated through the myoplasm to the site of entry, ATP-dependent SERCAs pump it back into the SR.

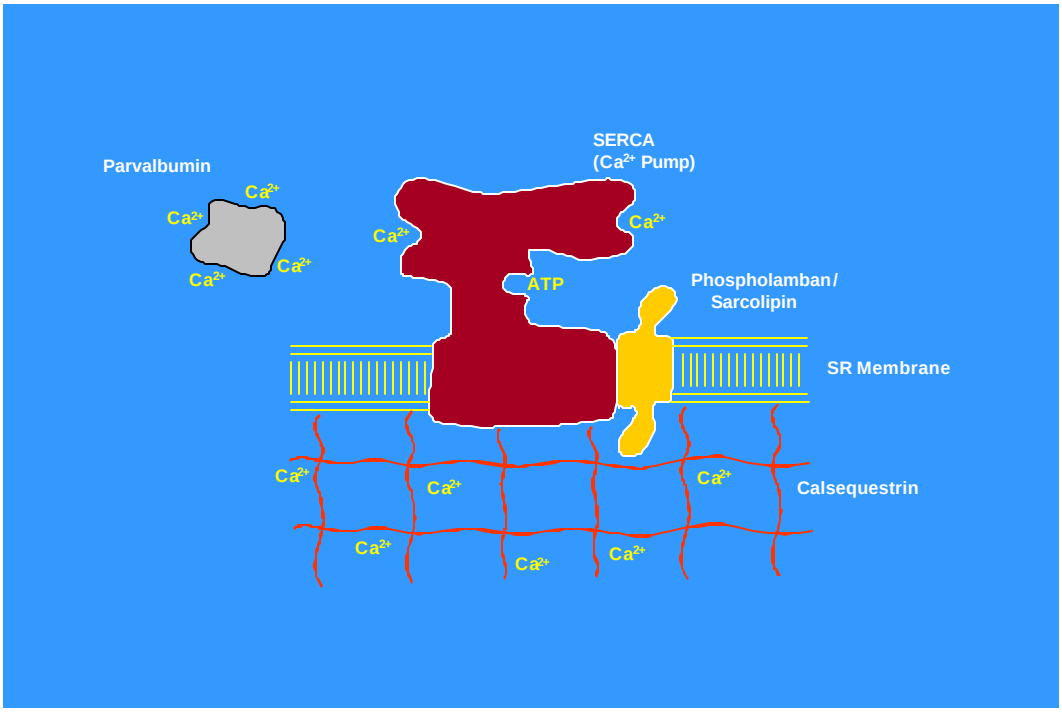

Figure 3: Diagram of the SR and proteins involved in Ca^{2+} uptake.

There are several different isoforms of SERCA, and their expression is tissue specific and developmentally regulated. SERCA1 is exclusively expressed in skeletal muscle—specifically fast-twitch skeletal muscle. SERCA2 is expressed in all tissues, muscle and non-muscle alike; however, it is found in higher levels in slow-twitch skeletal muscle (Berchtold et al., 2000). While several different isoforms exist, all SERCA function in essentially the same way. It is believed that upon binding ATP, a conformational change occurs in the protein. It is this change that allows Ca^{2+} to be transported across the SR membrane. One mole of enzyme binds and transports 2 moles of Ca^{2+}. Once inside the SR, Ca^{2+} is bound inside the organelle by the major storage protein

CSQ. This low-affinity and high-capacity protein completes Ca^{2+} cycling by binding the ion at the site of uptake and storing it in the SR. The function of CSQ is to buffer Ca^{2+} in the SR and keeps the free ionic Ca^{2+} concentrations low (Berchtold et al., 2000).

In summary, ECC is the process by which skeletal muscle contracts. It is initiated by a wave of depolarization that passes over the sarcolemma and down the T-tubules into the muscle fiber. The depolarization signal is transmitted from the voltage-sensitive DHPR to the RyR via mechanical coupling. Ca^{2+} is released from RyR into the myoplasm of the muscle fiber where it binds to TnC. Upon binding to TnC, contraction is initiated in the myofibrils. Relaxation is initiated when Ca^{2+} dissociates from TnC. In fast-type muscle fibers, Ca^{2+} is transported in part by PARV to the site of uptake into the SR. Using ATP as its energy source, SERCA pumps Ca^{2+} back into the SR. Ca^{2+} cycling is completed with the binding of Ca^{2+} by CSQ.

Abnormal Calcium Handling. Normal homeostasis of $[Ca^{2+}]_i$ is fundamental for proper regulation of Ca^{2+}-dependent skeletal muscle functions, including contraction. A number of disease states of striated and smooth muscle cells are the result of alterations in Ca^{2+} transients and elevated resting Ca^{2+} levels (Kargacin and Kargacin, 1996). Early DMD studies focused on muscle cell Ca^{2+} accumulation and how it was altered in dystrophic animals. Observations of elevated Ca^{2+} within these animals were integral in forming the hypothesis that Ca^{2+} ion regulation was altered in DMD. Turner et al. (1988) investigated $[Ca^{2+}]_i$ in skeletal muscle in adult normal and mdx mice. Measurements were made on

single intact fibers isolated from the flexor digitorum brevis muscle from the hind foot of mice. The fibers were microinjected with a solution of fura-2, a fluorescent dye that facilitates measurement of intracellular Ca^{2+} levels spectrophotometrically. Using this approach, $[Ca^{2+}]_i$ was found to be markedly elevated in mdx muscle fibers compared with normal fibers both at rest and during stimulation. It was also observed that Ca^{2+} transient kinetics were slowed in mdx fibers, and $[Ca^{2+}]_i$ levels remained elevated significantly longer in mdx fibers when they were stimulated at physiological frequencies. The slowed transient kinetics (i.e., slowed Ca^{2+} uptake) could explain the increased myoplasmic Ca^{2+} levels. Finally, protein degradation in mdx fibers was increased in response to elevated $[Ca^{2+}]_i$ (Turner et al., 1988).

Fong et al. (1990) observed similar elevations in $[Ca^{2+}]_i$ measured in normal versus dystrophic myotubes from human and mouse 6 to 15 days after myoblast fusion. Resting $[Ca^{2+}]_i$ levels in mdx mouse and Duchenne's human myotubes were significantly elevated compared to values obtained from normal mouse and human myotubes. When exposed to a tenfold increase in extracellular Ca^{2+} concentration, mdx myotubes showed a dramatic increase in $[Ca^{2+}]_i$, while normal mouse myotubes showed no significant change. Therefore, the ability to regulate $[Ca^{2+}]_i$ was compromised in dystrophic myotubes (Fong et al., 1990). Fong et al. explained the increases in $[Ca^{2+}]_i$ were due to a class of Ca^{2+} leak channels in the myotubes. The open probability of these leak channels was markedly increased in dystrophic myotubes. These results suggested that an increase in the activity of Ca^{2+} leak channels in dystrophic myotubes

contributed to elevations in $[Ca^{2+}]_i$ (Fong et al., 1990; Turner et al., 1991). The results presented in these studies provided insight into possible physiological changes that occur after but not prior to the onset of dystrophy in mdx muscles.

Turner et al. (1991) observed that resting $[Ca^{2+}]_i$ levels were elevated above control levels in areas located near the sarcolemma in mdx myotubes. The authors hypothesized that Ca^{2+} was leaking into myotubes through leak channels and this was contributing to higher $[Ca^{2+}]_i$ in mdx myotubes. To test this idea, the authors used the leak channel agonist nifedipine and found both leak channel activity and $[Ca^{2+}]_i$ were significantly increased. In addition, the DHPR receptor blockers verapamil and diltiazam did not lower resting $[Ca^{2+}]_i$ in dystrophic myotubes. This suggested that DHPR was not contributing to high levels of Ca^{2+} in the dystrophic myotubes and that it was the result of Ca^{2+} leaking into myotubes through leak channels. Nevertheless, no mechanistic connections have yet been made between the absence of the DGC and increased activity of leak channels.

A leaky sarcolemma or increased activity of leak channels may not be the only mechanisms by which $[Ca^{2+}]_i$ could rise to abnormal levels. The previous studies that investigated leak channel activity also noted changes in Ca^{2+} transient kinetics. Turner et al. (1988) observed slowed transient kinetics in mdx fibers. If $[Ca^{2+}]_i$ levels remained elevated significantly longer in mdx fibers when they were stimulated at physiological frequencies it could indicate that the problem actually lies in the Ca^{2+} cycling system involved in ECC. Turner et al. (1991) observed prolonged kinetics in mdx myotubes and hypothesized that this

could arise from a problem with Ca^{2+} sequestration, release, or both. Nicolas-Mentral et al. (2001) hypothesized that if Ca^{2+} handling was dysregulated in DMD, the contractile properties of dystrophic muscle should also be affected. In their study, myotubes were obtained from primary cultures of hind leg muscles of 1-3-day old mdx or control mice. Cells were used 2-3 weeks after fusion and 4 days after spontaneous contraction developed. Cellular excitability of the muscle cells was described as rheobase and chronaxy, variables determined from a plot of intensity (voltage) vs. stimulation duration (e.g., see Fig. 2A, Nicolas-Mentral et al., 2001). Typically, voltage decreases as stimulation duration increases, but eventually plateaus. Rheobase represents this plateau and is the minimal voltage required to induce contraction when stimulation duration is prolonged. Chronaxy is the duration that corresponds to a voltage that is twice the rheobase. The results of both measures showed heterogeneous distribution and there were no significant differences (of rheobase or chronaxy) observed between the responses of the mdx myotubes and the control myotubes. Contraction and relaxation rates were determined by measuring the time interval between 10 and 90% of the amplitude of contraction and relaxation. While there were no differences in rheobase, there were prolonged contraction and relaxation rates observed in mdx myotubes compared to control myotubes (approximately 138% and 167% longer respectively). Although Ca^{2+} transients were not measured along with contraction dynamics, it was concluded that the slowed contraction-relaxation process in dystrophic muscle was evidence of a dysregulation of Ca^{2+} homeostasis (Nicolas-Mentral et al., 2001). For example, a decreased capacity

for calcium removal in mdx cells could have accounted for the alterations in increased time of muscle cell relaxation.

De Luca et al. (2001) demonstrated that the ECC mechanism could be altered in dystrophin-deficient mouse muscle. Rheobase measurements were made during the degeneration process in mdx mice at 8-10 weeks, and again at 6-8 months. In mdx mice aged ≥ 4 months, muscle fibers needed significantly less depolarization to contract than wild-type animals of the same age; that is, the rheobase voltage was shifted toward more negative values (De Luca et al., 2001). As noted above, rheobase represents the minimum activation voltage for a prolonged duration of stimulation, but more specifically it represents the voltage where an equilibrium is attained between the speed at which Ca^{2+} is released and then buffered (De Luca et al., 2001). The authors concluded that the shift to a lower rheobase value could be due to elevated $[Ca^{2+}]_i$ in the muscles of mdx mice, and this could result from an increased release of Ca^{2+} and/or a reduction in Ca^{2+} uptake by the SR (De Luca et al., 2001). To test for reduced uptake, DeLuca et al. (2001) stimulated SERCA pumps in EDL muscles of wild-type and mdx mice with taurine, an amino acid that is present in muscle cells (~28 μmol/g) (Huxtable and Bressler,1973). Taurine exerts a protective action against cellular Ca^{2+} overload by stimulating Ca^{2+} pumps (Satoh and Sperelakis, 1998). It was hypothesized that the application of taurine to dystrophic muscle would alleviate problems with Ca^{2+} homeostasis that may be present at an older age in the mdx muscle by stimulating a faster uptake of Ca^{2+} and normalizing $[Ca^{2+}]_i$ in the muscles of mdx mice. If *in vitro* application of taurine at millimolar concentrations

significantly improves ECC in dystrophic muscle, this could be indicative of a problem in the uptake mechanism at the SR membrane. This was a possibility in the mdx muscle fibers used by De Luca et al. (2001), as taurine application significantly restored the ECC of dystrophic fibers to near normal values (De Luca et al., 2001). One problem with this interpretation is that the high concentrations (mM) used in taurine application may not be physiologically relevant. Although this study showed alterations in the ECC of dystrophic mice at ages ≥ 4 months, it did not definitively show that the differences in ECC were the result of altered uptake/release mechanisms.

If Ca^{2+} release rates are faster than normal and/or if Ca^{2+} continuously leaks from the SR faster than it can be recovered by SERCA in dystrophic muscle, the result could also be an increase in the myoplasmic concentration of Ca^{2+}. This could be the result of functionally altered uptake and release proteins. Leberer et al. (1988) investigated SR Ca^{2+}-uptake, the content and catalytic properties of SERCA, and the content of calsequestrin in muscle samples from control and mdx mice from birth to age 36 weeks. Ca^{2+}-uptake rates were determined with Ca^{2+}-sensitive electrodes in pooled muscle homogenates. Up to the age of 6-weeks, Ca^{2+} uptake rates in dystrophic muscle did not differ significantly from those observed in normal muscle. Thereafter, there was a marked decrease in the uptake rate observed in mdx muscle homogenates. In 22-week-old dystrophic animals, the uptake rate decreased enough to resemble those rates seen in 10-day-old control animals and represented a 50-70% reduction in Ca^{2+} uptake rates in mdx mice from higher levels obtained during

early maturation. Although the uptake activities were slowed in mdx muscle homogenates, there were no significant differences in the SERCA content between mice genotypes. There was a gradual and significant decline in the content of calsequestrin in dystrophic fast and slow muscles after 5-weeks of age. Impairment in Ca^{2+} sequestration was paralleled by a reduction in Ca^{2+} transport activity in dystrophic muscle and the defects appeared to manifest themselves progressively during development (Leberer et al., 1988). Still, it remained unlikely the alterations in sequestration of Ca^{2+} by the SR were possible causes for the initiation of dystrophy because the differences occurred after 5 weeks of age in the mdx mice. Thus, because the dystrophic changes begin in mdx mice between 3-4 weeks of age (Leberer et al., 1988), the alterations in uptake of Ca^{2+} were very likely secondary effects in response to an initial pathogenic insult.

Kargacin et al. (1996) hypothesized a blunted Ca^{2+} uptake mechanism was a possible cause for altered Ca^{2+} handling in skeletal muscle SR vesicle preparations from 8-week-old mdx mice. When compared to normal mice, the Hill coefficients (a measure of the affinity of an enzyme for its substrate) and Ca^{2+} sensitivity were the same. However, the maximum velocity of uptake, when normalized for the amount ATPase content of the vesicles, was less for the mdx mice. To normalize for SERCA content, the density of the SERCA protein band was divided by the summed densities of the total protein loaded on an SDS-PAGE gel. Kargacin et al. (1996) demonstrated that slower uptake could elevate myoplasmic Ca^{2+} concentrations in 8-week-old mice.

The uptake mechanism alone may not be the only SR function that is affected in the dystrophic condition. Takagi et al. (1992) used single skinned muscle fibers to investigate contractile regulation in skeletal muscle of control and mdx mice with special emphasis placed on the Ca^{2+} cycling by the SR. In this study, single muscle fibers were isolated from the tibialis anterior (TA) of mice aged 4-8 weeks. The fibers were skinned, stretched to 1.1 times slack length, and subjected to a contraction protocol. Fibers were first incubated in solutions of radiolabeled Ca^{2+} at different pCa values to obtain a profile of SR Ca^{2+} release at various submaximal and maximal Ca^{2+} concentrations. When the profile was complete, contraction was induced with caffeine. Various measures were obtained during and after contraction including: maximum force generated during contraction, Ca^{2+} uptake rate of the SR, rate of Ca^{2+}-induced Ca^{2+} release (CICR), and rate of Ca^{2+} leakage from the SR. Uptake rates of the radiolabeled Ca^{2+} did not differ between genotypes, and there were no differences observed in the rate of CICR. Ca^{2+} leaked at a significantly faster rate in mdx fibers, and, because inhibitors to caffeine such as procaine or Mg^{2+} had no effects on leakage, it is likely that the leakage was independent from CICR. There were differences in the dose-response relationship of caffeine contractures between the control and mdx fibers. For example, at various submaximal caffeine concentrations, the peak tension developed was higher in mdx muscle fibers (e.g., contracture at 2mM caffeine was significantly larger in mdx). Takagi et al. (1992) hypothesized that the already elevated Ca^{2+} levels in close proximity to the SR contributed to abnormal caffeine sensitivity. Although unconfirmed, the

increased leakage of Ca^{2+} via the RyR could have also contributed to the higher $[Ca^{2+}]_i$ in these dystrophic muscle fibers (Takagi et al., 1992). Takagi et al. (1992) did not comment on how mdx muscles could have adapted to maintain a homeostatic state in light of the increased leakage from their SR. It is possible, however, that increased Ca^{2+} uptake could compensate for the increased Ca^{2+} release into the myoplasm of the dystrophin-deficient muscle cells. Unfortunately, these measurements were not made, and these homeostatic adaptations could not be confirmed.

Not all studies have demonstrated alterations in $[Ca^{2+}]_i$ in dystrophic mouse models. McArdle et al. (1994) studied the uptake of radiolabeled Ca^{2+} by muscles and liver of control and mdx mice aged 14 days, prior to the onset of the dystrophic process. McArdle et al. (1994) found no differences in the $^{45}Ca^{2+}$ muscle/liver ratio in mdx and control mice. These results demonstrated there were no significant elevations in $[Ca^{2+}]_i$ in the myoplasm of mdx mouse muscle fibers at age 14 days. Conversely, mdx mice aged 40 days evaluated after the onset of dystrophy, demonstrated a significant increase in the $^{45}Ca^{2+}$ muscle/liver ratio, indicating an increase in $[Ca^{2+}]_i$ in the myoplasm. McArdle et al. (1994) hypothesized, therefore, that the accumulation of Ca^{2+} in dystophic muscle was a secondary effect of the degeneration process.

Collet et al. (1999) measured $[Ca^{2+}]_i$ with the fluorescent indicator indo-1 in single skeletal muscle fibers that were isolated from hindlimb muscles of mdx and control mice aged ~2-50 weeks. The mice used in this study provided insight into possible changes in myoplasmic Ca^{2+} levels in dystrophic muscle

before and after the onset of disease. No significant changes were noted in initial $[Ca^{2+}]_i$ between control and mdx fibers; in fact, in fibers from older (~35 weeks) mice, resting $[Ca^{2+}]_i$ was slightly higher in control mice than in mdx. After measuring resting $[Ca^{2+}]_i$, short depolarizing pulses were used on the fibers to elicit changes in $[Ca^{2+}]_i$. Again, similar properties were shown in fibers from both animals. There were significant elevations observed in the mean time constant of $[Ca^{2+}]_i$ decay following twitches of 5 ms duration in mdx fibers as compared to control fibers; however, for pulses longer than 5 ms, no significant differences were detected. Overall, Collet et al. (1999) showed that muscle fibers of mdx mice aged 2-50 weeks were capable of handling Ca^{2+} normally at both rest and during depolarization (Collet et al., 1999). Furthermore, it is of particular interest to note that at age 2 weeks, there was no difference in $[Ca^{2+}]_I$ for muscle fibers of mdx compared to those of control mice. This suggests that myoplasmic Ca^{2+} levels were not altered at this stage of maturation, and therefore not prior to the onset of dystrophic changes.

Khammari et al. (1998) found no significant alterations in SR Ca^{2+} uptake rates in mdx mouse diaphragm muscle. Late in the life of an mdx mouse, the degenerative dystrophic process begins to affect the diaphragm (Hoffman et al., 1988). Khammari et al. (1998) investigated SR Ca^{2+} handling in 7- to 8-week-old control and mdx mice, using a method known as rapid cooling contractures (RCCs). This approach provides an estimation of SR Ca^{2+} content and indicates how $[Ca^{2+}]_i$ is redistributed between intracellular binding sites and within the SR. Overall, the RCC data showed no differences in the rate at which Ca^{2+} was taken

up from the myoplasm (i.e., uptake by SERCA) in 7- to 8-week-old mdx mouse diaphragm compared to controls. The results of Khammari et al. (1998), demonstrated no significant alterations in Ca^{2+} cycling in dystrophin-deficient mice. These results differ from earlier results obtained from kinetic studies on Ca^{2+} handling in mdx mice (Turner et al., 1988; Kargacin et al., 1996). This divergence may be attributed to differences in the muscles selected for study or differences in methods to determine $[Ca^{2+}]_i$ (Khammari et al., 1998). It should again be noted that the age at which the animals were studied (~7-8 weeks) makes it difficult to draw conclusions about the role of Ca^{2+} in the onset of the dystrophic process, which occurs at approximately 3-4 weeks in mdx mice (Leberer et al. 1988).

Studies that measure Ca^{2+} kinetics are helpful to determine if uptake and release mechanisms are functionally altered in dystrophic compared to control muscle. If alterations are observed in intracellular Ca^{2+} handling, it follows that protein profiles of major Ca^{2+}-handling proteins in dystrophic muscle should also be investigated. Butcher et al. (1986) isolated SR from the hindlimb muscles of dystrophic and control mice aged 3 months. The protein contents of various Ca^{2+} handling proteins were assessed using SDS-PAGE. The investigators found that the protein content of Ca^{2+}-ATPase (i.e., SERCA) and calsequestrin were decreased in dystrophic compared to control muscles, providing some evidence for altered Ca^{2+} handling in dystrophic muscle (Butcher et al., 1986). For example, with less SERCA available to pump Ca^{2+} back into the SR, Ca^{2+} uptake rates could be reduced.

Pereon et al. (1997), determined gene expression of DHPR in diaphragm and tibialis anterior (TA) muscles from 9-11 week old mdx and control mice based on mRNA levels. No differences in gene expression of the skeletal muscle isoform of DHPR were noted between the control and mdx TA. In contrast, there were significant increases in DHPR mRNA expression in the mdx compared to the control diaphragm. To assess the functional significance of the increased DHPR gene expression, a high-affinity radiolabeled probe was used to quantify functional DHPRs. The probe worked by binding functional DHPR in muscle homogenates. Following that, the bound molecules were filtered and functional DHPRs were counted with a scintillation counter. There were no differences in the amount of functional DHPRs in mdx compared to control muscle. These data suggested that increased gene expression of DHPR in mdx diaphragm did not lead to increases in the content of functional DHPR in dystrophic muscle. If excess Ca^{2+} is not entering muscle cells due to increased expression of DHPRs, then increases in myoplasmic Ca^{2+} must be due to other factor(s) (e.g. leaking through membrane or from the SR).

In a similar study investigating protein content in dystrophic muscle, Culligan et al. (2001) observed no significant differences in the content of DHPR, SERCA, RyR, and calsequestrin in 8-week-old control and mdx mice. The only significant differences observed were those of calsequestrin-like proteins (CLPs) of molecular weight 150-220 kDa, where the content of these proteins in mdx mouse muscle were depressed to ~25-50% of control. The role these proteins play in Ca^{2+} binding is still unclear; however, if CLPs do aid in the sequestration

of Ca^{2+} in the SR, this decline could explain the decreased Ca^{2+} binding observed in dystrophin-deficient microsome preparations. If Ca^{2+} cannot be sequestered effectively in the SR, its concentration may be elevated in the cytoplasm.

A number of studies suggest that there are several mechanisms in dystrophic fibers that could ultimately lead to increases in $[Ca^{2+}]_i$. Calcium may enter through the sarcolemma at abnormally high levels via Ca^{2+} leak channels in dystrophin-deficient fibers. The SR may also elevate calcium within these muscle cells due to slowed Ca^{2+} uptake and/or faster Ca^{2+} release. Although the studies noted above indicate there is considerable controversy about Ca^{2+} homeostasis in dystrophic muscle and at what age potential changes might occur, it is quite probable that $[Ca^{2+}]_i$ if elevated, will have deleterious effects within muscle fibers.

Deleterious effects of increased $[Ca^{2+}]_i$. Calcium must be carefully regulated in the myoplasm of muscle fibers. For example, calpains are Ca^{2+}-dependent cysteine proteases within muscle cells. They are of particular interest in the etiology of DMD, as their concentration and activation may increase in response to higher $[Ca^{2+}]_i$ (Tibdall et al., 2000; Alderton and Steinhardt 2000). In addition, mitochondria, a primary source of energy for muscle cells, may also be targeted by increases in $[Ca^{2+}]_i$.

Activation of calpains. Calpains are a family of Ca^{2+}-dependent, cysteine proteases. There are several classes of calpains that differ in their structure; however, they all have similar fundamental biological functions (Tidball

& Spencer, 2000). The two ubiquitous calpain isoforms (μ- and m-calpain) are dependent on Ca^{2+} for activation and require approximately ~50 and ~300 μM, respectively, *in vitro* for activation (Hosfield et al., 2001). Normal concentrations of Ca^{2+} available in the myoplasm of a muscle cell are significantly lower (<1 μM) than those required experimentally for calpain activation (Hosfield et al., 2001); however, a Ca^{2+} overload in the myoplasm of dystrophic muscle could activate calpains and promote the degeneration of muscle fibers through increased proteolysis (Tidball & Spencer, 2000). Mdx mice experience an increase in total calpain concentration after the disease process begins (Spencer et al., 1995). A second study by Spencer et al. (1996) reported changes in calpain distribution throughout muscle fibers undergoing necrosis in mdx mice. Degenerating fibers had more diffusely distributed and less membrane-bound calpain compared to that of control fibers. This suggested widespread calpain auto-proteolysis in the mdx fibers (Spencer et al., 1996).

An *in vivo* study by Badalamente et al. (2000) tested the effectiveness of leupeptin, a calpain inhibitor, to delay or even prevent the necrosis commonly associated with muscle fibers of mdx mice. In this study, fourteen-day-old mdx mice were given intra-muscular injections of leupeptin twice daily for 30 days. After 30 days, hindlimb and diaphragm muscles were harvested from the mice. Histological analysis was performed to assess the amount of muscle degeneration in treated and untreated animals. Animals that did not receive the leupeptin treatment had significantly more degenerating and regenerating muscle fibers than animals receiving the treatment. A calpain activity assay also

revealed significant decreases in muscle calpain activity for leupeptin-treated compared to untreated mdx mice (Badalamente et al., 2000). The observed changes in expression, localization, and activation of calpains in mdx muscle support the hypothesis that calpain contributes to increased proteolysis in dystrophic muscle. Furthermore, the findings also demonstrated the possible negative effects of elevated $[Ca^{2+}]_i$ on muscle fibers.

Alterton and Steinhardt (2000) investigated the possibility that transient disruptions in muscle cell membranes eventually lead to degeneration via chronic increases in Ca^{2+}-dependent proteolysis. It was hypothesized that increased proteolysis was the result of elevated intracellular Ca^{2+} from Ca^{2+}-leak channels. Fluorescent substrates were used to determine calpain proteolysis *in vitro*; these were used in conjunction with Ca^{2+}-leak channel inhibitors. To investigate how contraction affected intracellular free Ca^{2+} levels, myotubes were cultured from control and mdx mouse muscles and allowed to contract. Mdx myotubes showed significant calpain substrate hydrolysis compared to control myotubes. This indicated a significant increase in activation of calpains, directly linked to contraction. When external Ca^{2+} was reduced to 0.09 mM from 1.80 mM in the cultures, the substrate hydrolysis rates decreased. Likewise, antagonists of Ca^{2+}-specific leak channels decreased substrate hydrolysis rates in mdx myotubes to near normal levels. Alderton and Steinhardt (2000) concluded that contraction-induced sarcolemmal injury in dystrophic myotubes begins a cascade of events, including abnormally active calcium-specific leak channels and accelerated calcium entry through these channels, which ultimately led to higher

levels of calcium-dependent proteolysis. The authors also commented that this series of events likely contributes to the death of muscle cells during the pathogenesis of muscular dystrophy (Alterton and Steinhardt, 2000). McCarter and Steinhardt (2000) further investigated the activity of Ca^{2+} leak channels near induced sarcolemmal ruptures in cultured myoblasts from 4-10-week-old adult mice. The mechanically induced ruptures were intended to mimic the tears that may naturally occur in muscle fiber membranes that lack dystrophin. Leak channel activity was examined near rupture sites (e.g., 5 microns from excision sites) and further from areas of micro-tears (e.g., 50 um away from ruptures). There was a marked increase in leak channel activity near rupture sites that was not observed in the presence of the protease inhibitor leupeptin. The authors concluded that increased Ca^{2+} leak channel activity was a result of proteolytic activity near sites of previous membrane ruptures. Furthermore, they hypothesized that this is what is occurring in dystrophic muscle. It was their hypothesis that, due to a general structural instability in the sarcolemma of muscle lacking dystrophin, there is a higher occurrence of membrane ruptures. This is followed by an influx of Ca^{2+} and an increase in Ca^{2+} dependent proteolysis. Finally, Ca^{2+} leak channels located near these ruptures are proteolytically activated—leading to a chronically elevated $[Ca^{2+}]_i$ in dystrophic muscle fibers. This new hypothesis represents a combination of the mechanical and calcium hypotheses, and suggests that there is, perhaps, not a single hypothesis explaining the onset of dystrophy during maturation.

In summary, while it is yet unclear if or when Ca^{2+} levels become elevated in dystrophic muscle, disrupted Ca^{2+} homeostasis in dystrophic muscle cells has the potential to give rise to increased activity of Ca^{2+}-dependent calpains. Several studies have reported increased activity of Ca^{2+}-dependent proteases in muscle fibers that lack dystrophin. This can have serious effects on the overall health of muscle cells and eventually lead to the widespread degradation observed in dystrophic muscle. With few studies available that demonstrate altered calcium handling in DMD during maturation, it cannot yet be concluded that the activation of calpains is a likely mechanism for the onset of the disease. Increased activity and potential proteolysis by calpains is a possible secondary effect in DMD, following an initial pathogenic insult.

Possible roles of mitochondria and cell death. In a recent review, Bernardi (1999) discussed the possible role that mitochondria play in the muscle fiber degeneration observed in DMD. Mitochondria are a primary source of energy for muscle cells through oxidative phosphorylation. They participate in intracellular Ca^{2+} signaling and contain pro-apoptotic proteins that can be released into the cytosol if normal cellular processes are disrupted (Bernardi, 1999). If Ca^{2+} becomes elevated in the myoplasm of dystrophic muscle fibers there is a possibility that mitochondria could be targeted, increasing the permeability transition (PT) state of these organelles. The end result could be influx of Ca^{2+} through the inner membrane of mitochondria, osmotic swelling, and finally, membrane rupture releasing pro-apoptotic molecules into the cytosol of affected muscle cells and initiating cell death (Bernardi, 1999). If Ca^{2+} levels are

truly elevated in DMD as is commonly believed, a compromise in mitochondrial function could occur early in the disease process of DMD.

Passaquin et al. (2002) demonstrated further evidence to support a mitochondrial role in DMD pathogenesis. To attenuate the impaired energy status in mdx muscle, newborn mdx mice were fed a creatine-enriched diet. Four weeks after birth, histological analysis revealed that the first wave of muscle necrosis in fast-twitch EDL muscles was dramatically reduced in mdx mice. There was a similar effect observed in slow-twitch hindlimb muscles; however these results were not significant. In gastrocnemius and soleus fibers isolated from mdx mice, supplemented with creatine for 8 weeks, the mitochodrial respiratory capacity (a measure of mitochondrial function) was significantly higher than that of untreated mdx and near that of control mice. Passaquin et al. (2002) suggested that the increase in cytosolic creatine levels stimulated mitochondrial respiration by increasing the efficiency of the mitochondrial enzyme creatine kinase. Normal mitochondrial function is imperative for muscle cell health, and damage to mitochondria could be severe enough to initiate cellular death through apoptosis. These studies suggest that mitochodrial dysfunction is seen in dystrophic mouse muscle after the onset of the disease and could be the direct result of perturbations in intracellular Ca^{2+} in these animals. However, much like calpain activation in onset of DMD, there is insufficient data to conclude that mitochondrial dysfunction is a likely mechanism for the onset of the disease. Any changes in mitochondrial function of dystrophic muscle are possible secondary effects in DMD, following an initial pathogenic insult.

Conclusion. Despite extensive research of DMD, its mechanism or mechanisms of onset are still unknown, although there are several hypotheses. The mechanical hypothesis, states that the loss of dystrophin and the DGC could weaken the muscle plasma membrane of muscle cells. It is commonly believed that the already weakened dystrophic membrane is more susceptible to injury during contraction and the injured membrane continues degrading as the disease progresses. A recent study suggests that the injury induced by contraction does not appear to initiate the dystrophic process in the muscles of maturing dystrophic mice (Grange et al., 2002).

The signaling hypothesis suggests that dystrophin and the DGC play a role in signal transduction between the cytosol and the extracellular matrix, and in their absence, the disrupted signaling may lead to ischemia and initiate as yet undetermined disease onset mechanisms. Because of the vast number of signaling pathways controlling normal physiologic function of a muscle cell, this is a particularly difficult hypothesis to explore. To date, there have been limited studies and it remains the least well understood and least supported of the hypotheses.

A subset of the signaling hypothesis, the Ca^{2+} hypothesis, is the focus of the current study. Current research indicates that perturbations in Ca^{2+} levels within dystrophic muscle may play a role in the initiation of DMD during early maturation. There is controversy over whether or not Ca^{2+} levels are abnormally high in muscle cells lacking dystrophin and how these higher levels arise. Some studies suggest that a less stable membrane (from the absence of dystrophin)

allows Ca^{2+} to pass into the myoplasm through Ca^{2+} leak channels. Other studies propose that the problem could arise from alterations in SR Ca^{2+} cycling. If there are alterations in the function or content of key proteins in Ca^{2+} cycling with the SR, Ca^{2+} levels could be affected. In many of the studies, the age of animals (i.e., after onset of dystrophy) has precluded drawing conclusions about the role of altered Ca^{2+} handling in the onset of the disease. If the mechanism of onset of the dystrophic process is of primary interest, animals must be used at an age before the overt signs of dystrophy.

Two critical elements that have contributed to the controversy over the role of Ca^{2+} in the onset of DMD are the model and age of the dystrophic mice. Thus, the purpose of this study was to determine if Ca^{2+} cycling by the SR was altered in maturing dystrophic mouse muscle (e.g., prior to weaning) in both mdx and mdx:utrn$^{-/-}$ mice. Notably, studies involving Ca^{2+} handling in the muscles of maturing mdx/utrn$^{-/-}$ mice have not yet been conducted, an important consideration, as they appear to be a better model than mdx mice for DMD.

Chapter 3: Methods

Mice. Control mice (C57BL/6), mdx mice, which lack dystrophin; and mdx:utrn$^{-/-}$ mice, which also lack utrophin (utrn) were used. Overt signs of muscular dystrophy occur at 2-3 weeks in mdx/utrn$^{-/-}$ mice (Grady et al., 1997) and 3-4 weeks in mdx mice (Carnwath and Shotton, 1987), yet the timing and the mechanisms that initiate DMD are not yet clearly defined. Previous studies have not targeted the early maturation period of mdx/utrn$^{-/-}$ or mdx mice; therefore this study investigated potential changes in calcium homeostasis in maturing mice (e.g., prior to weaning).

The Animal Use and Care Committee of Virginia Tech approved all procedures used in this study. Mice were housed at the Virginia Tech Laboratory Animal Resource Facility. Animals were allowed to both eat (Purina Rodent Laboratory Chow) and drink water *ad libitum* and were exposed to a 12-hour light/dark cycle. To determine the mouse genotype (e.g., mdx or mdx:utrn$^{-/-}$), PCR analysis was performed on DNA isolated from tail snips using established procedures (Grange et al., 2002). Tissue was obtained from anaesthetized mice at two ages: 9-10 days and 21 days. In each age group, muscle samples from 5-6 mice of each genotype were assessed.

Muscle Homogenate Preparation Protocol. The quadriceps muscles from both male and female mice were used for all experiments. Mice were anesthetized with ketamine/xylazine (intraperitoneal injection of 2 mg xylazine and 20 mg Ketamine per 100 g body mass). Following deep anesthesia, muscles were rapidly excised, and then the mouse was euthanized by intra-

cardiac injection of ketamine/xylazine. Muscle homogenates were prepared using a method modified from Williams et al. (1998). After a brief mincing, the muscles were homogenized with three, 15-second bouts (VirTis VirTishear) in 10 volumes of homogenization buffer (10 ml per gram of muscle wet weight). For the smaller muscles of the 9-10 day group, 15 volumes of homogenization buffer were used. The buffer contained 20 mM N-[2-hydroxyethyl] piperazine-N'-[2-ethane-sulfonic acid] (HEPES), 0.2% sodium azide (NaN_3), 300 mM sucrose and 100mM ethylenediaminetetraacetic acid (EDTA). To improve the yield of intact proteins in the homogenate fraction, a protease inhibitor cocktail (Sigma) was added at a dilution of one ml of cocktail solution to 100 ml of homogenate. The inhibitor cocktail contained a mixture of protease inhibitors with broad specificity for the inhibition of serine, cysteine, aspartic and amino-peptidases. Specifically, the cocktail solution contained the following concentrations of inhibitors: AEBSF, 104 mM; aprotinin, 0.08 mM; leupeptin 2.1 mM; bestatin 3.6 mM; pepstatin A, 1.5 mM; and E-64, 1.4 mM. The samples were centrifuged at 1,600 g for 10 minutes in a Beckman centrifuge, the supernatant removed and frozen at -80° C, and the pellet was discarded. Because sucrose serves to protect the membrane integrity of the SR during freezing, the samples could be safely stored in the homogenization buffer until analysis.

Protein Concentration Assay. The protein concentration of each muscle homogenate was determined using modified methods of Bradford et al. (1976). Bio-Rad protein dye (Bio-Rad) was mixed 1:4 with water, and 2.5 mls of the dilution was added to individual cuvettes. Approximately 10 µl of homogenate

supernatant was added to the protein dye solution in the cuvette, briefly vortexed, and allowed to incubate for approximately 5-10 minutes. The absorbance of each homogenate sample was measured at 595 nm (Milton Roy, Spectronic 1001 Plus spectrophotometer), and the absorbance was converted to a protein concentration using a standard curve. The standard curve was generated from absorbance readings of 10, 20, 30, and 40 μM concentrations of Bovine Serum Albumin (BSA).

	Group 1 (9-10 days)		
	Muscles homogenized/SR isolated and stored in 300 mM sucrose		
	Control	*Mdx*	*Mdx:utrn*$^{-/-}$
Measurements	SR calcium uptake SR calcium release SERCA content Ryanodine receptor content Parvalbumin content Calsequestrin content	Western blot SDS PAGE	

	Group 2 (21 days)		
	Muscles homogenized/SR isolated and stored in 300 mM sucrose		
	Control	*Mdx*	*Mdx:utrn*$^{-/-}$
Measurements	SR calcium uptake SR calcium release SERCA content Ryanodine receptor content Parvalbumin content Calsequestrin content	Western Blot SDS PAGE	

Table 1. The experimental groups and measurements obtained after tissue collection and storage.

SR Ca^{2+} Uptake. The rate of Ca^{2+} uptake into the SR of homogenate fractions was measured using an HP 8453 UV-visible spectroscopy system (Hewelett Packard). The homogenate fractions contained a crude mix of cellular proteins and intact SR vesicles that retained the ability to take-up and release Ca^{2+}. The presence of Ca^{2+} outside the vesicles was measured using the metallochromatic dye antipyrylazo III. Two hundred μg of homogenized protein was added to 1.5 ml of Ca^{2+} uptake buffer containing the following: 100mM potassium chloride (KCl), 20 mM N-[2-hydroxyethyl] piperazine-N'-[2-ethane-sulfonic acid] (HEPES), 1mM magnesium chloride ($MgCl_2$), 10 mM potassium oxalate, 1 mM adenosine Triphosphate (ATP), and 50 mM antipyrylazo III (APIII). The buffer was equilibrated to 37° C in 1-cm^2 cuvettes in a water bath. Sample cuvettes were then transferred to the spectrophotometer for analysis. After collecting a brief period of baseline data for approximately 10 seconds in the absence of Ca^{2+}, 15 μl of 4 mM $CaCl_2$ stock solution was added to the uptake buffer, and data were collected for approximately 160 seconds. Uptake rates were computed from the steepest negative slope over consecutive 10-point data sets after the addition of $CaCl_2$. The slope was determined with a linear-fit over the 10-point data sets, and the steepest slope taken as the maximal uptake value. A standard curve was formed by determining the absorbance of 1.5 mls of uptake buffer in a 1 cm cuvette while adding consecutive aliquots of 0.02 μM $CaCl_2$ stock solution to 0.10 μM. Uptake rates were expressed as mg of Ca^{2+} per μg of protein per minute. This is a uniform way of expressing Ca^{2+} uptake, and facilitated comparison between groups (Williams et al., 1998).

Sodium Dodecyl Sulfate Polyacrylamide Gel Electrophoresis and Western Analysis. The content of several key proteins involved in Ca^{2+} cycling were determined in the muscle samples using Western analysis, including: SERCA1 and SERCA2, the isoforms of the ATP-dependent Ca^{2+} pump; CSQ, a protein which sequesters Ca^{2+} in the SR lumen after uptake; PARV, a protein which facilitates transport and uptake of Ca^{2+} by the SR; and RyR1, the major channel for Ca^{2+} release from the SR of skeletal muscle. Primary mono- and polyclonal antibodies were used to identify specific proteins following gel electrophoresis and protein transfer. Protein content was determined for each sample by visualizing with secondary antibodies conjugated with horseradish peroxidase (HRP) and quantifying by densitometric analysis. Using this "snapshot" of protein content, comparative analyses were then made between mouse genotypes and between age groups.

Muscle samples were placed in 2x sample buffer containing the following: 240 mM β-mercaptoethanol, 1 M Tris (pH 6.8), 20% glycerol, 0.01% bromophenol blue, and H_20. Samples were diluted (1 μg/μl SR protein) with water and then combined in a 1:1 ratio with the sample buffer. The final concentration of the samples in the sample buffer was 0.5 μg/μl. The samples were boiled for 2 minutes and stored at -80° C until use.

Sodium dodecyl sulfate polyacrylamide gel electrophoresis (SDS-PAGE) was performed on the samples using the method of Laemmli (1970) in a mini-PROTEAN® III cell apparatus from Bio-Rad. In this method, polymerization of monomers of acrylamide crosslinked with bis-acrylamide form a porous gel that

allows proteins to migrate in inverse proportion to molecular weight when subjected to an electric field. If the percentage of bis-acrylamide is kept constant in all gels, the size of pores in a gel is inversely proportional to the percentage of acrylamide used in the solution. If the percentage of acrylamide is high in solution, the size of the pores in the gel will be smaller and visa versa. Separating gels made with the same percentage of bis-acrylamide and different percentages of acrylamide were used to separate proteins according to their size. A 4% "stacking gel" overlaid on the separating gel orders or "stacks" the proteins contained in each sample by size (smallest first) before they subsequently enter the separating gel. For assessment of each protein, the same stacking gel composition was used, but the separating gel composition was varied. A 7.5% separating gel was used to separate both SERCA 1 and 2. A 5% separating gel was used to separate RyR, a 10% gel was used to separate CSQ, and a 15% gel was used to separate PARV. The recipes for each gel are shown in Table 2.

SDS Gels	**4% Stacking**	**5%**	**7.5%**	**10%**	**15%**
Stock Component (mls)					
Distilled H_20	6.34	12.3	10.93	9.68	7.18
1.5 M Tris, (pH 8.8)	--	5.0	5.0	5.0	5.0
0.5 M Tris (pH 6.8)	2.5	--	--	--	--
10% SDS	0.10	0.20	0.20	0.20	0.20
Acrylamide 40%	1.0	2.5	3.75	5.0	7.50

Table 2. Reagents and volumes of various separating gels of different percentages (5-15%).

Polymerization occurs most efficiently in the absence of oxygen; therefore, the stacking and separating gels were degassed in a vacuum for 20 minutes. To begin the polymerization process, 20 µl of 97% N,N,N',N'-tetramethylethylenediamine (TEMED) and 100 µl of 10% ammonium persulfate (APS) were added to a given separating gel solution. The solution was gently mixed, poured into the mini-PROTEAN® III cell to a level 1 cm below the lip of the small glass plate, then overlaid with 20% ethanol. The gel was allowed to polymerize for at least 30 minutes. After polymerization, the ethanol was poured off and 0.1% SDS was used to wash the top of the gel and glass plates. For all SDS-PAGE gels, a 4% stacking gel solution was prepared and degassed in the vacuum for 20 minutes. Polymerization was initiated by adding 20 µl of TEMED and 100 µl of 10% APS. The stacking gel solution was gently mixed and poured over the polymerized separating gel, and the lane combs were placed between the two glass plates. The glass plates were placed in the electrophoretic apparatus to form the upper chamber. The stacking gel was allowed to polymerize for 30 minutes. When polymerization was complete the combs were removed and electrode buffer was added to the upper chamber of the apparatus. The electrode buffer contained the following: 3-g/l TRIS base, 24-g/l glycine, and 3 g/l SDS. On each gel, one well was loaded with approximately 7 µl of broad-range molecular weight markers (BioRad). Each of the remaining wells was loaded with 15 µg of SR protein in sample buffer. Following loading and before turning the apparatus on, the bottom chamber was also filled with electrode buffer. Except for RyR, the protein gels were run at a constant 200 V until the

bromophenol blue tracking dye ran off the gel (approximately 1 hr). For RyR, the running conditions were set at 45 mA, and the gels were run for approximately 2 hrs.

Protein	Voltage Settings	Run time (min)
SERCA 1	30 V (constant)	960
SERCA 2	30 V (constant)	960
RyR	30V (constant)	1080
CSQ	100 V (constant)	60
PARV	100 V (constant)	30

Table 3. Voltage settings and run times for transfer of various proteins.

Western Transfer. A electrophoretic run was considered complete when the tracking dye ran off the gels. The gels were removed from the mini-PROTEAN® apparatus and placed in transfer buffer for 40 minutes. The nitrocellulose (NC) membrane (BioRad) and filter paper were cut to 48 cm^2 (i.e., 6 cm x 8 cm, the approximate dimensions of the separating gel) and equilibrated in transfer buffer for approximately 15 minutes. The transfer buffer consisted of 10% 10x transfer buffer, and 20% pure Methanol brought to a final volume of 1 liter with distilled water. The final 1x transfer buffer contained the following: 0.192 M glycine, 25 mM TRIS, and 1.73 mM SDS. A Bio-Rad Mini Trans-Blot® Electophoretic Transfer Cell was used to transfer proteins from the gels to the NC sheets. The transfer sandwich was initiated by placing the cassette, with the black side down, on a clean surface. Next, one pre-wetted fiber pad was placed on the black side of the cassette. Two pre-wetted sheets of filter paper (BioRad) were placed on top of the fiber pad. Then the equilibrated gel was placed on the

filter paper, and a pre-soaked NC membrane was placed on the gel. To complete the sandwich, two more sheets of pre-wetted filter paper and a fiber pad were placed on top of the membrane. To avoid artifacts from air trapped between the different sandwich layers, a glass tube was used to gently roll out the air bubbles. The cassette was oriented in the tank so the negatively charged proteins would migrate onto the NC towards the positively charged electrode in the tank. The tank was filled with transfer buffer, a stir bar added, and was placed on a stir table to help maintain even buffer temperature. The various run times and voltage settings for optimal transfer of proteins are reported in Table 3.

After the transfer was complete, the NC sheets were removed, placed in a plastic dish, and washed 3 times in Tris Buffered Saline + 0.05% Tween 20 (TTBS) at room temperature for 10 minutes per wash. The NC sheets were then placed in a blocking solution composed of 5% non-fat dry milk (NFDM) in TTBS. The sheets were agitated on a shaker in the blocking solution for approximately 2 hrs at room temperature. The NC sheets were then incubated overnight at 4°C with a specific primary antibody in 5% NFDM/TTBS. The various antibodies and dilutions used for primary incubation are listed in Table 4.

After incubation in the desired primary antibody, the NC sheets were again washed 3 times in TTBS at room temperature for 10 minutes per wash. The NC membranes were incubated in Horseradish peroxidase-conjugated (HRP) AffiniPure-Goat Anti-Mouse IgG (Jackson ImmunoResearch Laboratories, Inc.) or Goat-Anti-Rabbit IgG depending on the host from which the corresponding primary antibodies were derived. The NC sheets were agitated in the secondary

antibody solutions of 5% NFDM/TTBS at a concentration of 1:5000 at room temperature for 1.5 hours. After this, the NC membranes were washed 3 times in TTBS at room temperature for 10 minutes per wash. The western blots were visualized using enhanced chemiluminescence (ECL). In this method, Chemiluminescent HRP substrates are used to make antibody-antigen complexes visible. To develop with ECL (Pierce), 2.5 mls of reagent A were mixed with 2.5 mls of reagent B. Each NC sheet was incubated in 5 mls of reagent mixture for 2 minutes. As recommended by the manufacturer, the approximate ratio of ECL reagent mixture to surface area of the NC membrane used for western blot was 0.125 mls of working solution per cm^2 of membrane. The NC sheets were then placed on a glass plate and covered with plastic wrap. The blots were exposed to film (Kodak) in a dark room. The length of time for development depended on the strength of the luminescence. For example, SERCA1 blots were exposed to film for 1 minute. Parvalbumin which had a much stronger signal was exposed to film for only a few seconds. The optical density of bands was determined using the 1D-Multi (Line Densitometry) function of the AlphaImager 2000 (v. 3.3b) program. The densities were measured over the full length of the each band. To normalize the content of a protein in each sample, the same amount of protein from a control sample was run on each gel and visualized with the Western protocol. The same control sample was used as a reference for each Western blot.

Protein	1º Antibody	Clone	Host	Manufacturer	[Conc]
SERCA 1	MA3-911	IIH11	Mouse	Affinity Bioreagents, Inc.	1:2500
SERCA 2	MA3-919	2A7-A1	Mouse	Affinity Bioreagents, Inc.	1:1000
RyR	MA3-925	34C	Mouse	Affinity Bioreagents, Inc.	1:5000
PARV	PC255L	Ab-1	Rabbit	Oncogene Research Products	1:4000
CSQ	MA3-913	VIIID12	Mouse	Affinity Bioreagents, Inc.	1:1000

Table 4. Antibodies and concentrations used for primary incubations in Western analysis.

2º Antibody	Host	Manufacturer	[Conc]
Peroxidase-conjugated AffiniPure Anti-Mouse IgG (H+L)	Goat	Jackson ImmunoResearch Laboratories, Inc.	1:5000
Peroxidase-conjugated AffiniPure Anti-Rabbit IgG (H+L)	Goat	Jackson ImmunoResearch Laboratories, Inc.	1:4000

Table 5. Antibodies and concentrations used for secondary incubations in Western analysis.

Coomassie Staining for Total SERCA. The amount of total SERCA present in the samples was determined using a 7.5% acrylamide SDS-PAGE gel that was run for 1 hour at a constant 200 V. Proteins were detected with a 0.1% Coomassie Blue solution containing: 0.1% Coomassie Blue R-250, 40% methanol, 10% acetic acid, and 49.9% distilled H_20. The gels were agitated in the solution overnight at room temperature in order to allow the dye to adequately bind to the proteins. The Coomassie Blue solution was poured off the gels and the background dye was removed from the gels with a destaining solution until a clear pattern of proteins could be seen. The destaining solution

contained 40% methanol, 10% acetic acid, and 50% distilled H_20. The 1D-Multi (Line Densitometry) function of the AlphaImager 2000 (v. 3.3b) program was used to determine the optical density of SERCA bands on the gels.

Statistics. A two-way ANOVA was used to compare uptake and release rates and protein content between genotypes and within each age group, as well as determine potential interactions between genotype and age. Differences between means were determined using Tukey's test, and were considered significant at $p < 0.05$. In the case that numerical data failed normality, and there were a significant number of samples within a genotype in which protein content was at a level too low to be detected, the numerical data was converted to a categorical form. Two-way ANOVA was used to analyze the categorical data with significant differences set at $p < 0.05$.

.

Chapter 4: Results

Mice. Analyses were performed on quadriceps muscles obtained from six normal mice (C57BL/6 strain), six mdx mice, and five mdx:utrn$^{-/-}$ mice at two ages: approximately 9.3 days (range: 9-10 days) and 21-days. At 9-10 days, the average weights of the control, mdx, and mdx:utrn$^{-/-}$ mice were 5.7-, 5.6-, and 6.0-g, respectively. At 21-days, the average weights of the control, mdx, and mdx:utrn$^{-/-}$ mice were 10.1-, 8.8-, and 10.1-g, respectively. At 9-10 days, the average weights of the pooled quadriceps of control, mdx, and mdx:utrn$^{-/-}$ mice were 33.3-, 39.9-, and 29.0-mg, respectively. At 21-days, the average weights of the control, mdx, and mdx:utrn$^{-/-}$ mice were 108.8-, 103.4-, and 98.4-mg, respectively.

Calcium Uptake Rates and Release Rates. Calcium uptake and release rates were determined in homogenates derived from quadriceps muscles obtained from control and dystrophic mice aged 9-10 days and 21 days. For mice aged 9-10 days, there was a 27.9% increase in the Ca^{2+} uptake rate for the mdx (0.612 ± 0.089 μmol/min/mg, $p < 0.05$) compared to the mdx:utrn$^{-/-}$ (0.333 ± 0.044 μmol/min/mg) genotype (Fig. 4). There was no difference in the uptake rates between the control (0.437 ± 0.059 μmol/min/mg) and the values for either of the dystrophic genotypes (Fig. 4). Similarly, at this age, there were no differences in the Ca^{2+} release rates between the genotypes (control: 0.223 ± 0.049 μmol/min/mg; mdx:0.292 ± 0.047 μmol/min/mg; mdx:utrn$^{-/-}$: 0.251 ± 0.039 μmol/min/mg).

For mice aged 21 days, there was a 73.1% and 61.3% increase in Ca^{2+} uptake for the mdx/utrn$^{-/-}$ genotype (1.432 ± 0.104 μmol/min/mg, $p < 0.05$)

compared to control and mdx genotypes (control: 0.701 ± 0.058 μmol/min/mg; mdx: 0.819 ± 0.065 μmol/min/mg) respectively (Figure 4). There were no differences in Ca^{2+} release rates between the genotypes at 21-days-of-age (control: 0.221 ± 0.019 μmol/min/mg; mdx: 0.205 ± 0.038 μmol/min/mg; mdx:utrn$^{-/-}$: 0.204 ± 0.054 μmol/min/mg).

When all genotypes were combined, there was a 52.3% increase in uptake rates from 9-10 to 21 days (9-10 days: 0.461 μmol/min/mg; 21 days: 0.984 μmol/min/mg $p < 0.05$). There was no significant interaction between genotype and age ($p > 0.05$) for Ca^{2+} release (Figure 5). There were no differences in release rates across age (9-10 days: 0.255 μmol/min/mg; 21 days: 0.212 μmol/min/mg; $p > 0.05$) (Fig. 5).

Coomassie Staining for Total SERCA. To determine total SERCA content, quadriceps muscle homogenates from quadriceps from control and dystrophic mice were run on a 7.5% SDS-PAGE gel. The gels were stained with Coomassie Blue and the AlphaImager program was used to measure the optical density of the single SERCA band of approximately 110 kDa. The optical density of the SERCA band for each sample was normalized using the same control sample run on each gel. Overall, there was a significant interaction between genotype and age ($p < 0.05$). However, there were no differences in total SERCA content between genotypes at 9-10-days-of-age (control: 0.500 ± 0.039 AU; mdx: 0.606 ± 0.038 AU; mdx:utrn$^{-/-}$: 0.464 ± 0.022 AU, $p > 0.05$) (Fig. 6). Similarly, there were no differences in total SERCA content between genotypes at 21-days-of-age (control: 0.896 ± 0.054 AU; mdx: 0.883 ± 0.056 AU; mdx:utrn$^{-/-}$:

1.013 ± 0.076 AU, p > 0.05) (Fig. 6). Within each genotype (control, mdx, mdx/utrn$^{-/-}$), there was an increase in the amount of total SERCA with age (p < 0.05). The optical density of bands on the Coomassie stained gels indicated that there was a 41.3%, 27.7%, and 39.6% increase in total SERCA content in control, mdx, and mdx/utr$^{-/-}$ mice respectively (Figure 6).

Western Analysis. Although all samples had some measurable total SERCA based on the Coomassie stained gels, SERCA isoforms were not detected in all samples using Western analysis (Appendix B). Overall, there was not a significant interaction between genotype and age (p > 0.05). There were no differences in SERCA 1 content between genotypes at 9-10-days-of-age (control: 0.117 ± 0.037 AU; mdx: 0.314 ± 0.076 AU; mdx:utrn$^{-/-}$: 0.051 ± 0.030 AU, p > 0.05) (Fig. 7). Similarly, there were no differences in SERCA 1 content between genotypes at 21-days-of-age (control: 0.779 ± 0.105 AU; mdx: 0.766 ± 0.106 AU; mdx:utrn$^{-/-}$: 1.044 ± 0.119 AU, p > 0.05) (Fig. 7). In all cases, within each genotype (control, mdx, mdx/utrn$^{-/-}$), there was a increase in the amount of SERCA 1 with age. The optical density of bands on the western blots indicated that there was a 66.2%, 45.2%, and 99.4% increase in the SERCA 1 content in control, mdx, and mdx/utrn$^{-/-}$ mice respectively (Figure 7).

The data obtained by measuring the optical density of bands on western blots for SERCA 2 failed tests for normality when two-way ANOVA was used to analyze the numeric data; therefore, the data was converted to a categorical form where SERCA 2 was determined to be “present” or “absent” from samples. Two-

way ANOVA was performed on the categorical data, and there was no statistically significant interaction between genotype and age using Tukey's test.

When expressed as categorized data and analyzed by ANOVA, there were no differences in the percentages of samples that contain SERCA 2 between genotypes at 9-10-days-of-age (control: 0.0%; mdx: 16.7%; mdx:utrn$^{-/-}$: 20%, $p > 0.05$) (Fig. 8). Similarly, there were no differences in the percentages of samples that contained SERCA 2 between genotypes at 21-days-of-age (control: 50%; mdx: 33%; mdx:utrn$^{-/-}$: 80%, $p > 0.05$) (Fig. 8). There not a statistically significant interaction between genotype and age ($p > 0.05$) (Figure 8). It should be noted that the absence of signal for SERCA 2 in the Western analysis could indicate (1) absence of protein, (2) presence of protein, but in quantities too low to be detected by the antibody, or (3) the antibody was not specific enough to SERCA 2 in the quadriceps homogenate samples.

Calsequestrin and PARV showed similar results—there were no significant interactions between genotype and age for protein content. There were no differences in CSQ content between genotypes at 9-10-days-of-age (control: 0.205 ± 0.057 AU; mdx: 0.173 ± 0.052 AU; mdx:utrn$^{-/-}$: 0.412 ± 0.102 AU, $p > 0.05$) (Fig. 8). Similarly, there were no differences in CSQ content between genotypes at 21-days-of-age (control: 0.634 ± 0.049 AU; mdx: 0.663 ± 0.087 AU; mdx:utrn$^{-/-}$: 0.717 ± 0.078 AU, $p > 0.05$) (Fig. 9). There was a 40.8% increase in CSQ content in 21-day-old animals from the 9-10-day-old animals (9-10 days: 0.263 AU; 21 days: 0.671 AU, $p < 0.05$) (Fig. 9).

There were no differences in PARV content between genotypes at 9-10-days-of-age (control: 0.624 ± 0.055 AU; mdx: 0.575 ± 0.067 AU; mdx:utrn$^{-/-}$: 0.608 ± 0.062 AU, $p > 0.05$) (Fig. 10). Similarly, there were no differences in PARV content between genotypes at 21-days-of-age (control: 0.982 ± 0.025 AU; mdx: 1.042 ± 0.049 AU; mdx:utrn$^{-/-}$: 0.920 ± 0.049 AU, $p > 0.05$) (Fig. 10). When all genotypes were combined, a 37.9% increase in parvalbumin content was detected in 21-day-old animals from the 9-10-day-old group (9-10 days: 0.602 AU; 21 days: 0.981 AU, $p < 0.05$) (Fig. 10). There were increases in CSQ and PARV with age but no differences between genotypes within each age group.

Western analysis of RyR1 yielded two distinct bands. It is commonly believed that one band (~ 565 kDa) is the skeletal muscle isoform of RyR, while the second band (~ 410 kDa) represents a proteolytic fragment (Wu et al., 1997). Therefore, on the RyR1 western blots, densities of both bands were summed to determine the total amount of RyR1 in each sample. There was no significant interaction between genotype and age ($p > 0.05$). There were no differences in the amount of RyR1 between genotypes at either age group (Figure 11). There were no differences in RyR1 content between genotypes at age 9-10 days (control: 0.305 ± 0.124 AU; mdx: 0.354 ± 0.097 AU; mdx:utrn$^{-/-}$: 0.283 ± 139 AU, $p > 0.05$) (Fig. 11). Similarly, there were no differences in RyR1 content between genotypes at 21-days-of-age (control: 0.513 ± .194 AU; mdx: 0.415 ± 0.138 AU; mdx:utrn$^{-/-}$: 0.568 ± 0.062 AU, $p > 0.05$) (Fig. 11). At each age, there was no difference in the amount of the 410-kDa proteolytic fragment between genotypes (Figure 11). There were no differences in 410-kDa fragment content between

genotypes at 9-10-days-of-age (control: 0.815 ± 0.180 AU; mdx: 0.549 ± 0.140 AU; mdx:utrn$^{-/-}$: 0.767 ± 0.244 AU, $p > 0.05$) (Fig. 11). Similarly, there were no differences in 410-kDa fragment content between genotypes at age 21 days (control: 1.392 ± 0.105 AU; mdx: 1.612 ± 0.221 AU; mdx:utrn$^{-/-}$: 1.495 ± 0.291 AU, $p > 0.05$) (Fig. 11). There was no interaction between genotype and age in the content of the 410-kDa proteolytic fragment ($p > 0.05$). The density of the 410-kDa proteolytic fragment bands increased with age, with an increase of approximately 78.9% in the fragment at 21-days-of-age from 9-10 days (9-10 days: 0.828 AU; 21 days: 1.500, $p < 0.05$). When the densities of both bands were summed, a significant difference was found between age groups (Figure 11). With the increase in age, there was a 59.8% increase in the amount of total RyR1 present (9-10 days: 1.194 AU; 21 days: 1.998, $p < 0.05$). As with SERCA 2, there were several samples in which no detectable bands for RyR1 were present. These results do not necessarily mean that there was no RyR1 channel present (Appendix B). As with SERCA 2 Western analysis, the protein could be present in levels too low to be detected by the antibody. Other possibilities are that (1) the epitope at which the antibody normally binds is damaged or (2) the calcium release channels could be present as isoforms that do not react with the 34C clone (i.e., RyR2).

Relation Between Protein Content and SR Uptake and Release Rates.

Densities for total SERCA and RyR1 were plotted against corresponding uptake or release rates, respectively, and assessed by a bivariate fit. When SERCA content was plotted against uptake rates, there was a significant positive

correlation ($r = 0.872$; $r^2 = 0.761$; $p < 0.05$). When RyR1 content was plotted against release rates, a weak relationship was revealed ($r = 0.296$; $r^2 = 0.088$; $p > 0.05$).

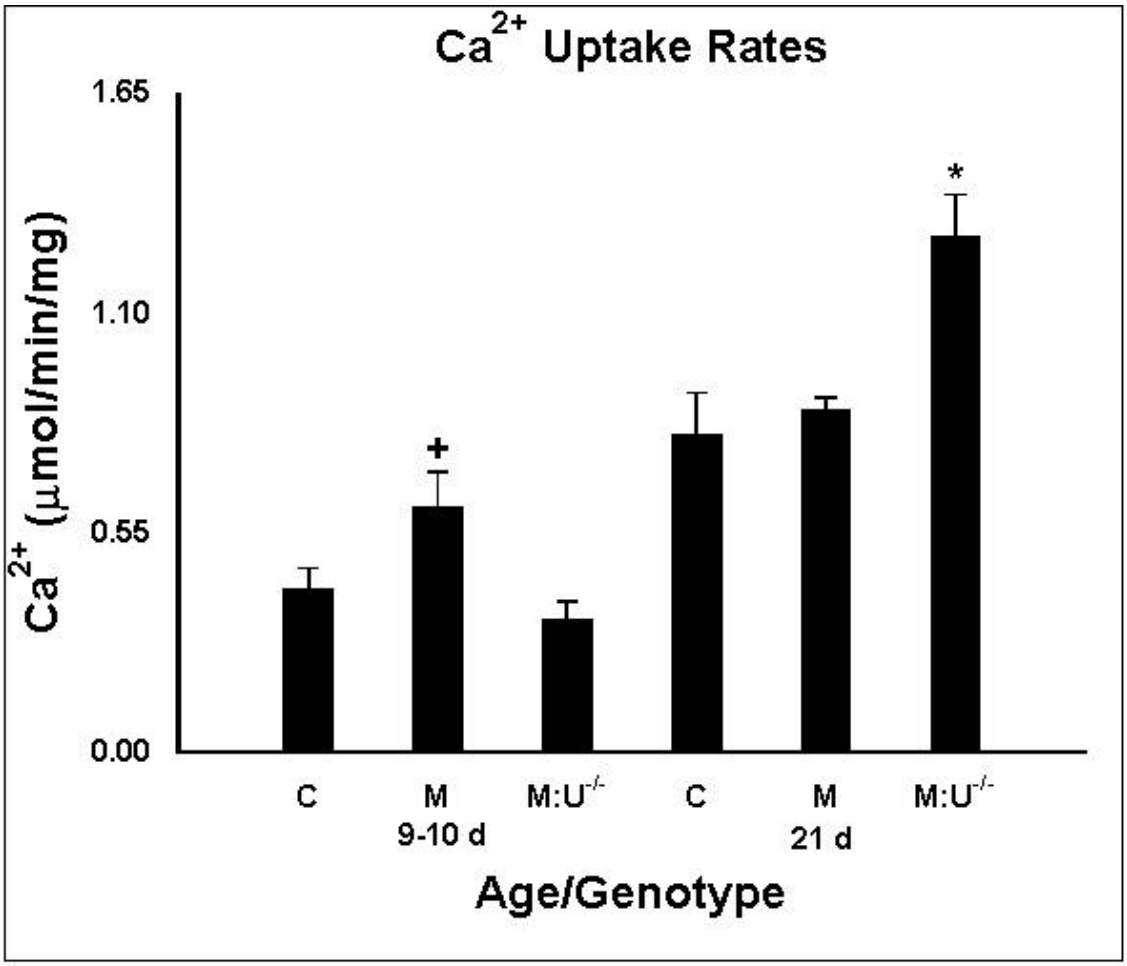

Figure 4: Mean uptake rates + standard error (SE) in control (C), mdx (M), and mdx/utrn$^{-/-}$ (M:U$^{-/-}$) mouse samples. * Significantly different from control ($p < 0.05$). $^{+}$ Significantly different from M:U$^{-/-}$ ($p < 0.05$).

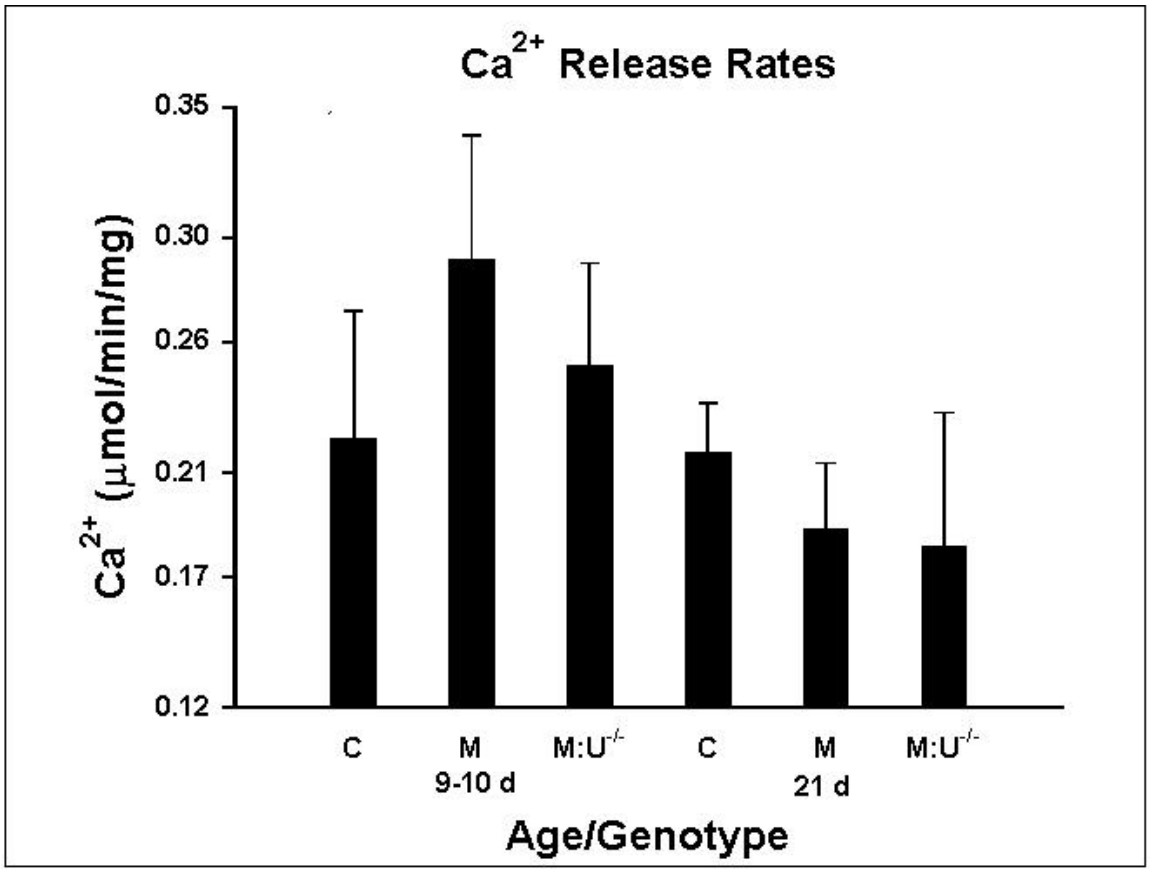

Figure 5: Mean release rates + standard error (SE) in control (C), mdx (M), and mdx/utrn$^{-/-}$ (M:U$^{-/-}$) mouse samples.

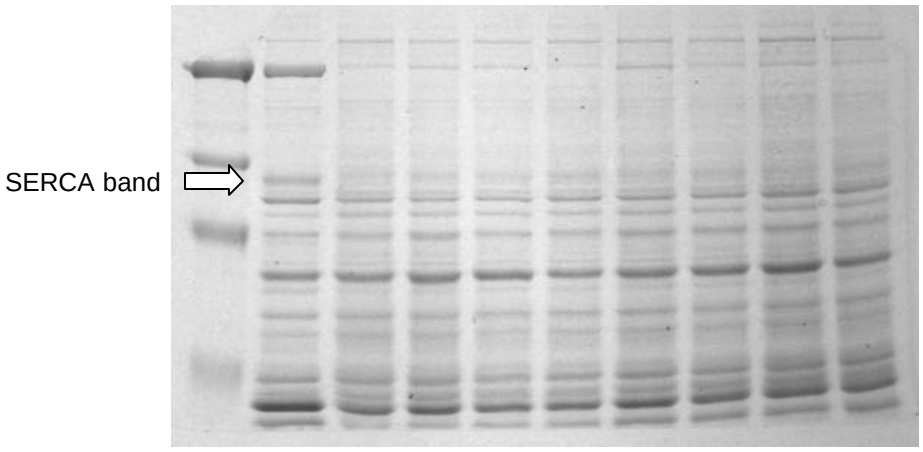

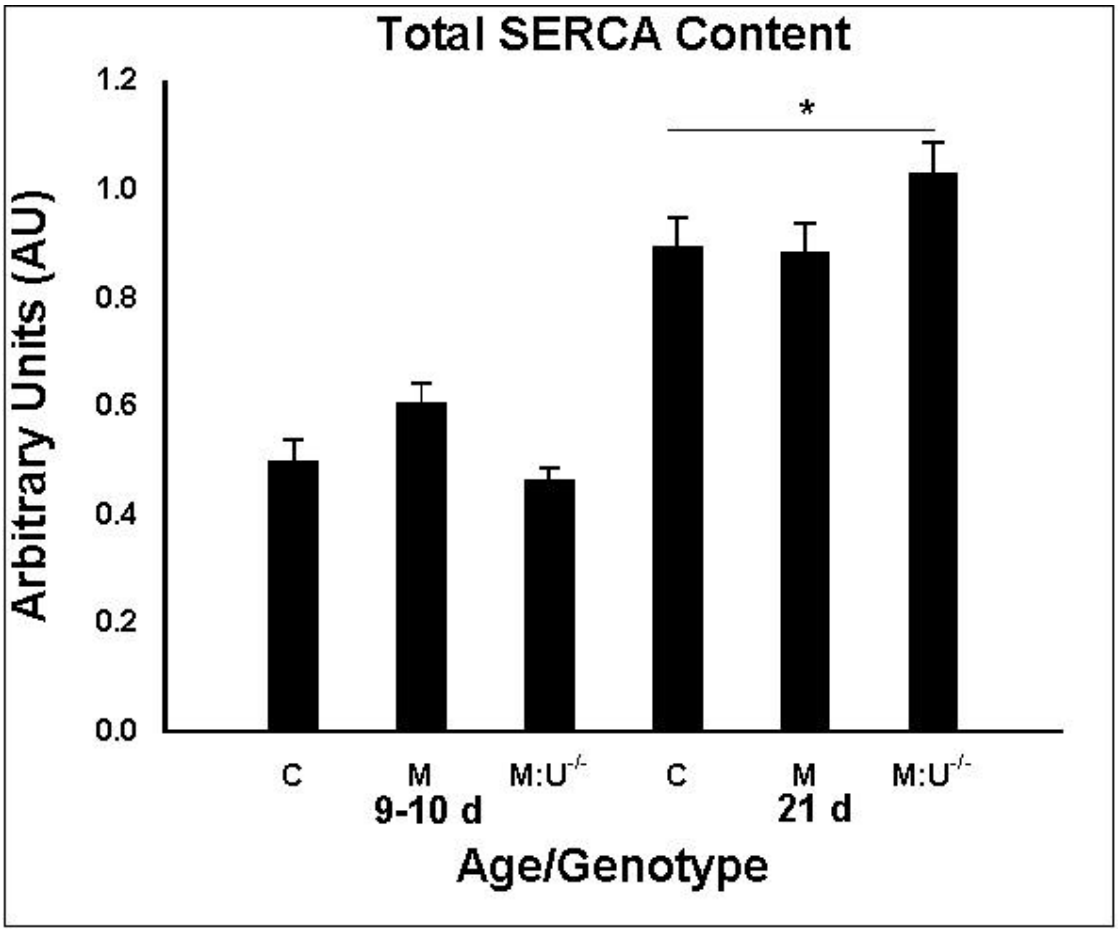

Figure 6: Total SERCA content in C, M, and M:U$^{-/-}$ mice at ages 9-10 days and 21 days. Top: Representative Coomassie stained gel. Bottom: Mean optical densities + standard error (in arbitrary units—AU). * Significant difference in SERCA content from younger age group ($p < 0.05$).

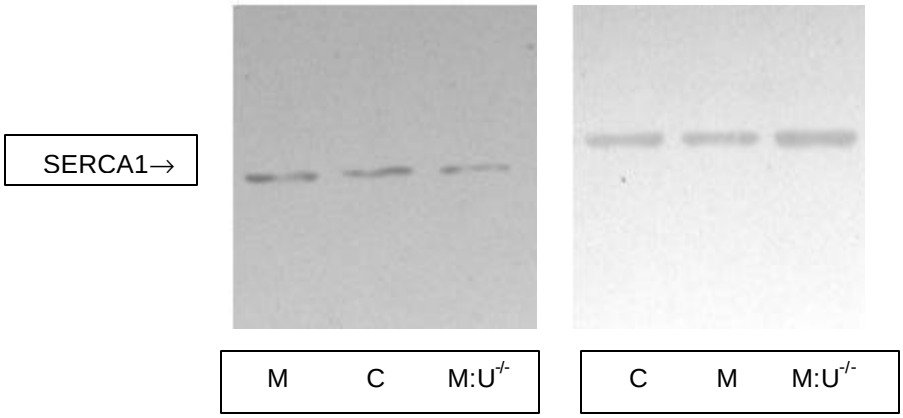

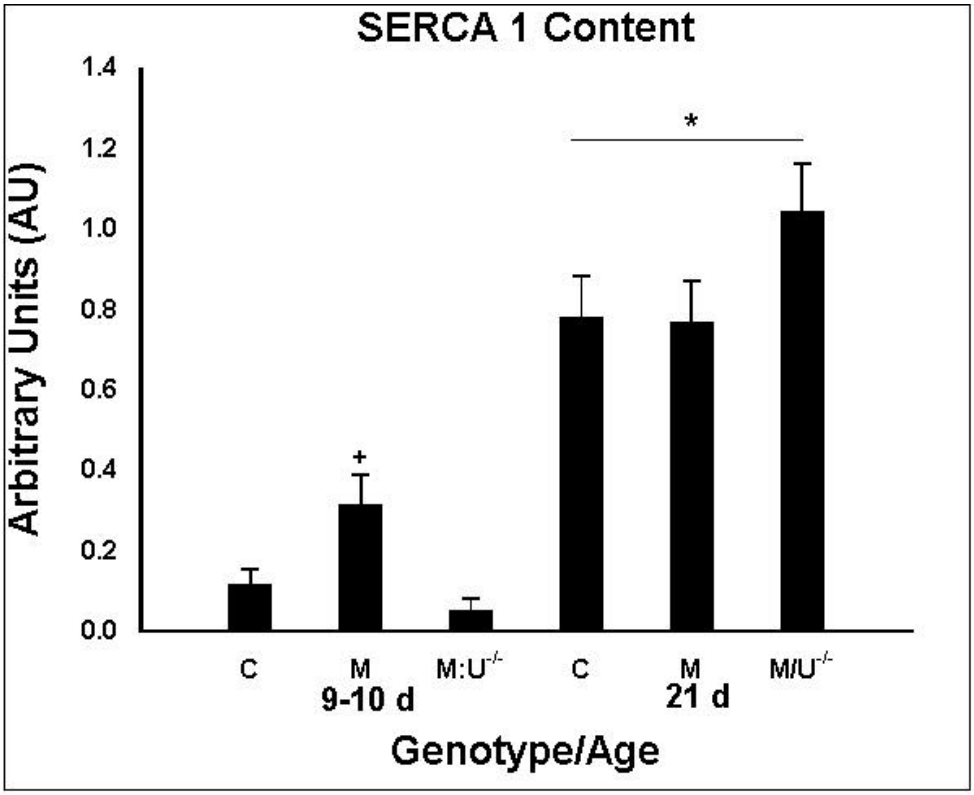

Figure 7: Western blot results for SERCA1 in C, M, and M:U$^{-/-}$ mice at ages 9-10 days and 21 days. Top left: Representative western blot of 9-10 day mouse samples using MA3-911 clone antibody. Top right: Representative western blot of 21 day mouse samples using MA3-911 clone antibody. Bottom: Mean optical densities + standard error (SE) (in arbitrary units—AU). * Significant difference in SERCA1 content from younger age group ($p < 0.05$). $^{+}$ Indicates significant difference from M:U$^{-/-}$ ($p < 0.05$).

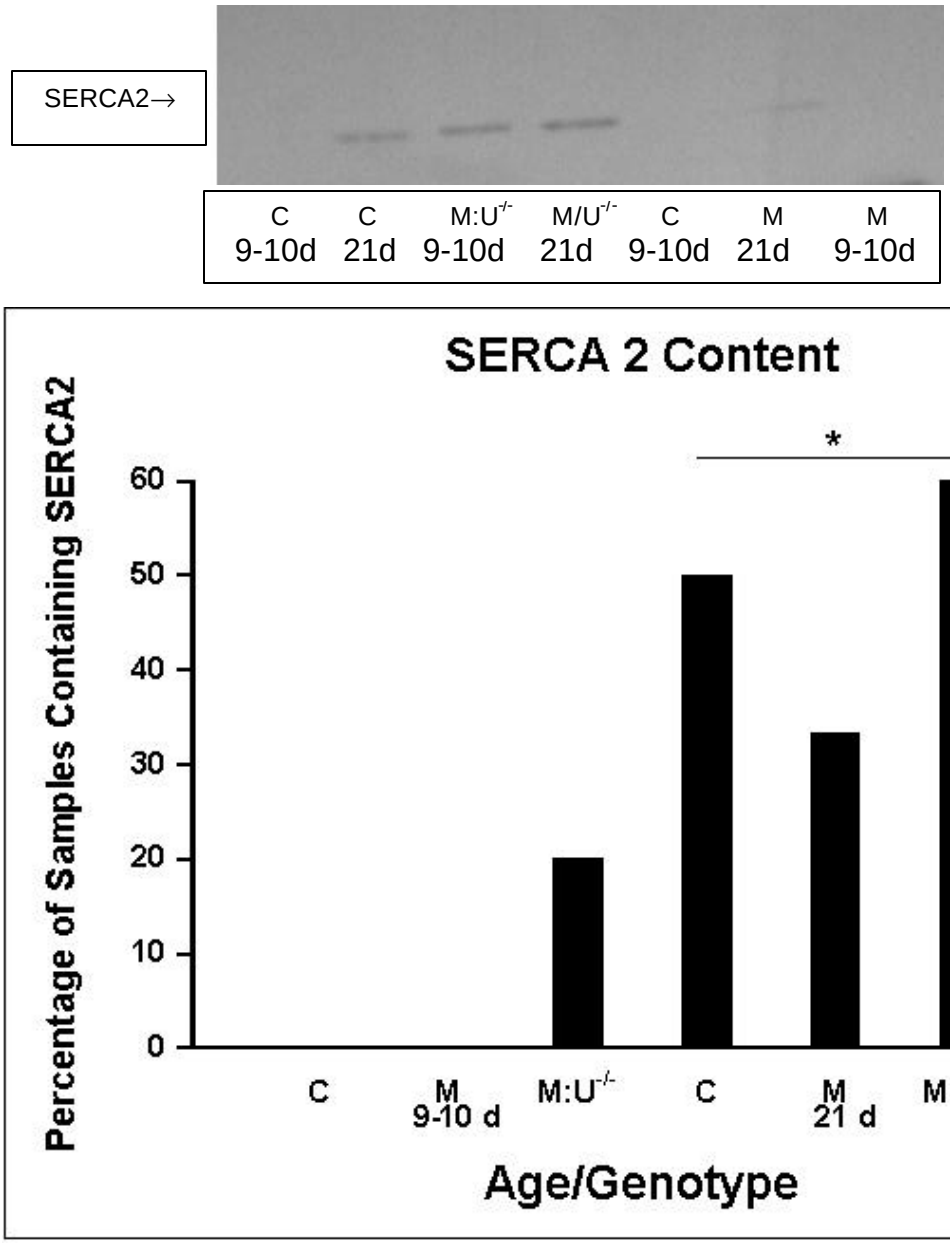

Figure 8: Western blot results for SERCA2 in C, M, and M:U$^{-/-}$ mice at ages 9-10 days and 21 days. Top: Representative western using MA3-919 clone antibody. Bottom: Mean optical densities + standard error (SE) (in arbitrary units—AU). * Significant difference in SERCA2 content from younger age group ($p < 0.05$).

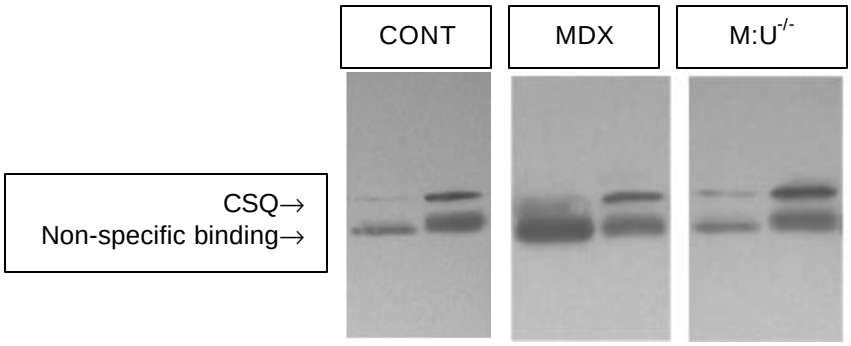

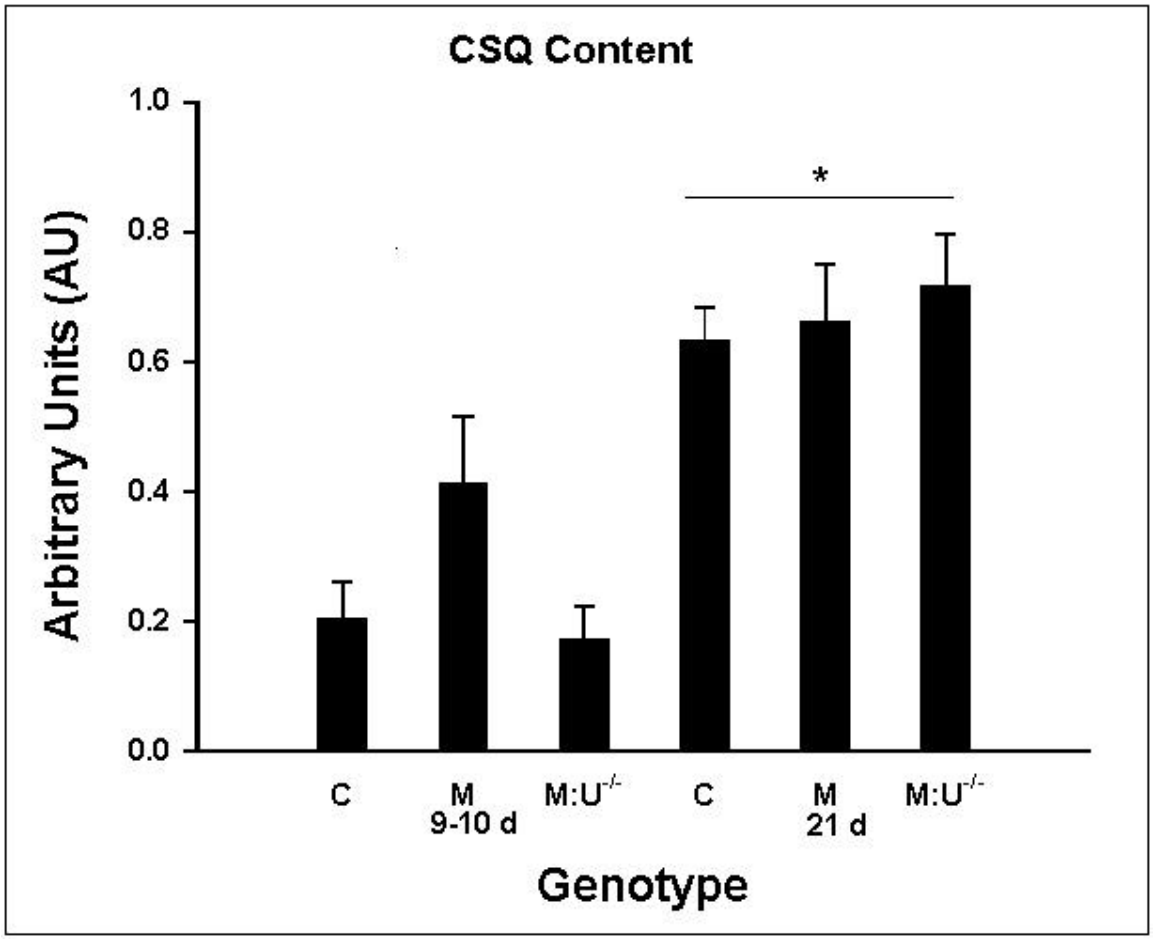

Figure 9: Western blot results for CSQ in C, M, and M:U$^{-/-}$ mice at ages 9-10 days and 21 days. Top: Representative western blots using VIID12 clone antibody. For each representative blot, 9-10 day samples appear on the left & 21-day samples appear on the right. Bottom: Mean optical densities + standard error (SE) (in arbitrary units—AU). *Significant difference in CSQ content from younger age group ($p < 0.05$).

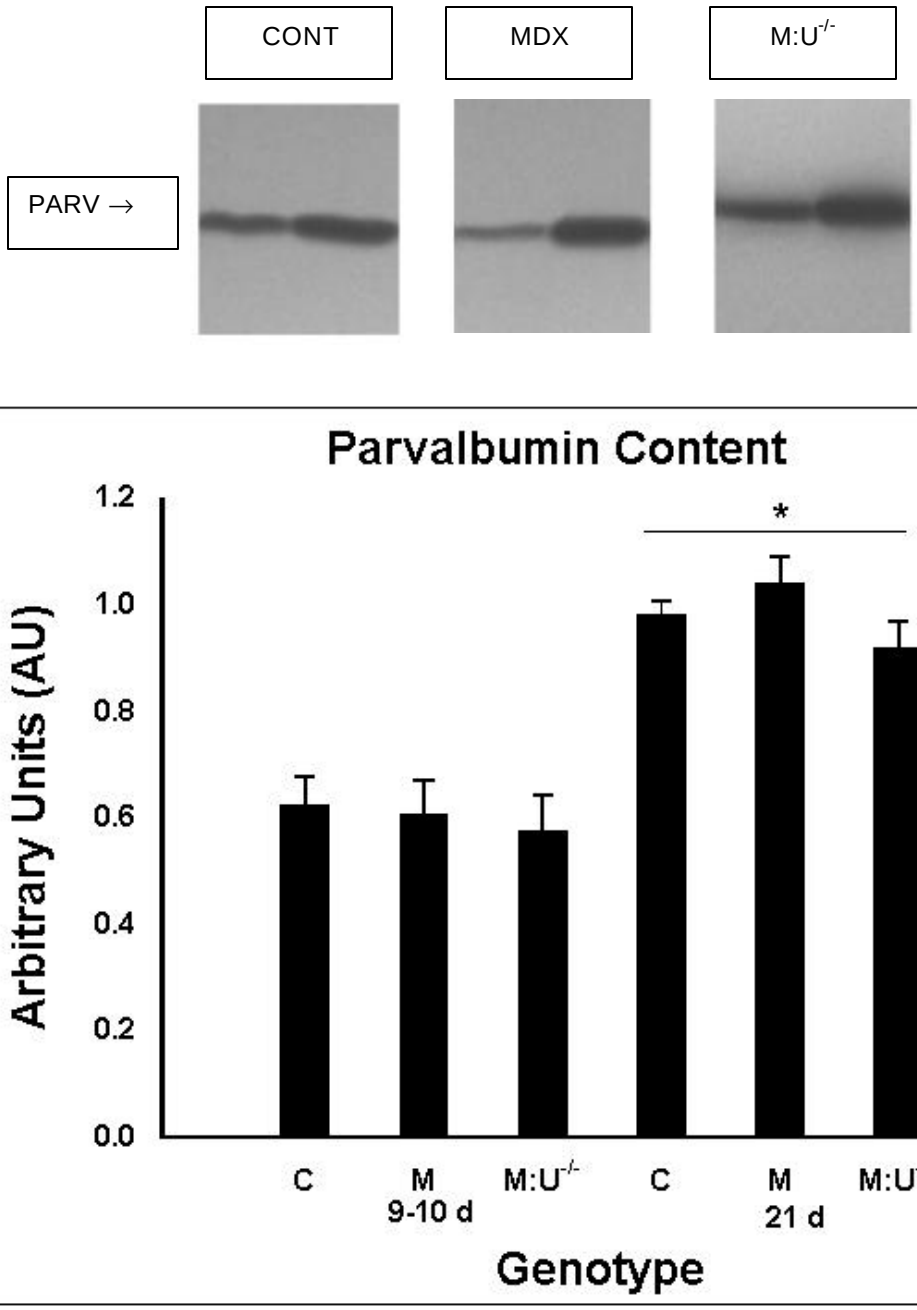

Figure 10: Western blot results for PARV in C, M, and M:U$^{-/-}$ mice at ages 9-10 days and 21 days. Top: Representative western using Ab-1 clone antibody. For each representative blot, 9-10 day samples appear on the left & 21 day samples appear on the right. Bottom: Mean optical densities + standard error (SE) (in arbitrary units—AU). * Significant difference in PARV content from younger age group ($p < 0.05$).

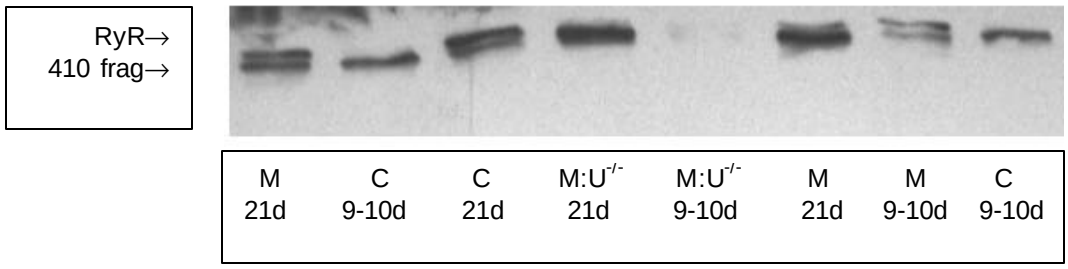

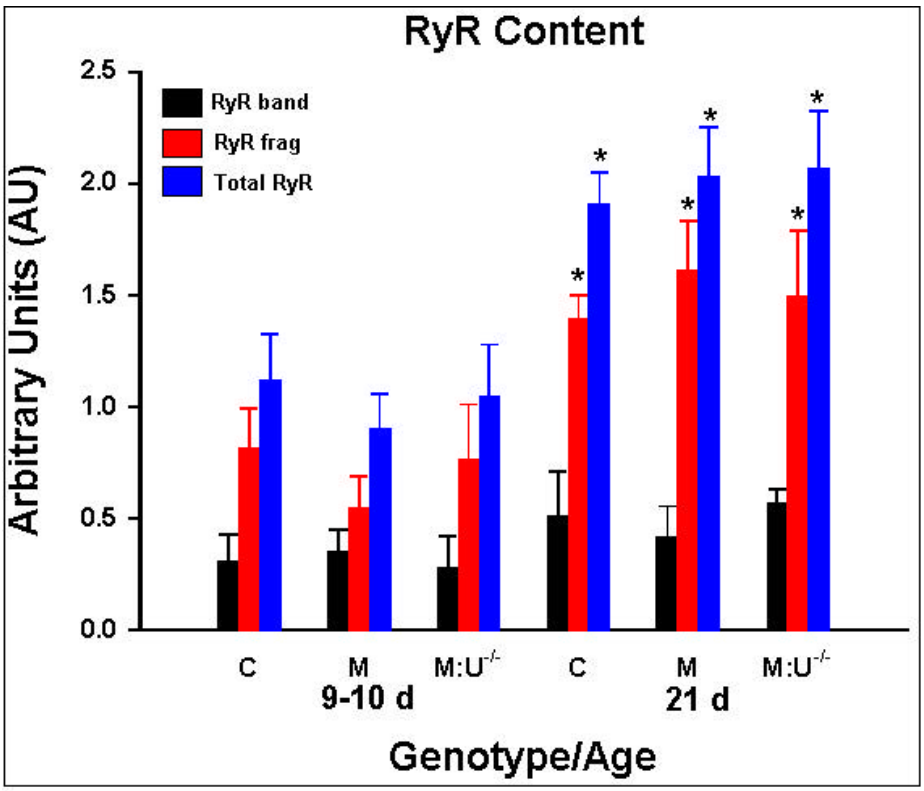

Figure 11: Western blot results for RyR1 in C, M, and M:U$^{-/-}$ mice at ages 9-10 days and 21 days. Top: Representative western blot using 34C clone antibody. Bottom: Mean optical densities + standard error (SE) (in arbitrary units—AU). * Significantly different from younger age group ($p < 0.05$).

Chapter 5: Discussion

The role of the SR in the onset of DMD is not presently known. An increased cytosolic Ca^{2+} concentration is believed to be a contributing factor in the initiation of DMD during early maturation, likely through Ca^{2+}-dependent proteolytic or apoptotic pathways (Turner et al., 1988, Fong et al., 1990). The increased $[Ca^{2+}]_i$ could result from leaky Ca^{2+} channels and/or a dysfunctional SR. This study focused on the potential role of the SR. There are two obvious deficiencies in the current literature to effectively address the SR as a source of the increased $[Ca^{2+}]_i$: (1) the age of the animals and, (2) the dystrophic model employed. First, the function of the SR has not been assessed in maturing skeletal muscle (i.e., prior to weaning), but rather in muscles of older animals during or following the dystrophic process. Second, investigators have relied primarily on the mdx mouse model, which may not be as representative of DMD as the mdx:utrn$^{-/-}$ mouse model. The purpose of this study therefore was to determine if Ca^{2+} cycling by the SR was altered in maturing dystrophic mouse mdx and mdx:utrn$^{-/-}$ skeletal muscle, which could then lead to abnormally high myoplasmic Ca^{2+} concentrations.

Major Finding. The major finding in this study was that the mean SR Ca^{2+} uptake rate for quadriceps muscles of mdx/utrn$^{-/-}$ mice aged 21 days was approximately 2-fold higher than the values for age-matched mdx and control mice. There were no differences in release rates at either age 9-10 or 21 days. Although most of the key Ca^{2+} handling proteins demonstrated increases in content as a function of age, no differences were observed at age 21 days to

account for the increased Ca^{2+} uptake rates. In general, at both age 9-10 and 21 days, the data suggest that there was little difference in the ability of the SR from either dystrophic model to cycle Ca^{2+}. However, the increased SR uptake rates in the mdx:utrn$^{-/-}$ muscles at age 21 days may represent an adaptation to increased $[Ca^{2+}]_i$, and/or changes in intrinsic SERCA function and/or regulation, to maintain cytosolic calcium concentration.

SR uptake but not release rates are altered in mdx:utrn$^{-/-}$ muscles.

Previous studies with older dystrophic muscle have revealed elevations in myoplasmic Ca^{2+} levels in muscle cells that lacked dystrophin (Turner et al., 1988; Fong et al., 1990). For example, slowed Ca^{2+} kinetics were observed in flexor digitorum longus muscles of adult mdx mice with Ca^{2+} levels markedly elevated above normal (Turner et al., 1988). A possible cause for this altered homeostatic state in muscles of older mice may have been changes in intracellular Ca^{2+} cycling such as increased release coupled with impaired uptake into the SR (Kargacin et al., 1996). Furthermore, changes in the content of specific Ca^{2+} handling proteins could alter Ca^{2+} cycling. Butcher et al. (1986) isolated SR from the hind limb muscles of dystrophic and control mice aged 3 months found that the protein content of SERCA and CSQ were decreased in dystrophic compared to control muscles, providing some evidence for altered Ca^{2+} handling in dystrophic muscle (Butcher et al., 1986). Recent studies with mice lacking the PARV gene demonstrated significantly longer half relaxation times than those observed in wild-type animals (Schwaller et al., 1999). This indicates Ca^{2+} uptake by the SR in the affected animals is slowed. In contrast,

Culligan et al. (2001) observed no significant differences in the content of DHPR, SERCA, RyR, and CSQ in control and mdx mice aged 8 weeks.

The uptake and release data observed in this study suggest SR calcium cycling is little changed in dystrophic compared to control muscles at age 9 days. At age 21 days, the mdx:utrn$^{-/-}$ mice, a more representative model of DMD, had significantly higher Ca^{2+} uptake rates than age-matched mdx or control mice. Some possibilities that may explain the higher Ca^{2+} uptake rates by the SR include higher content of SERCA, PARV, and RyR, lower content of CSQ, or altered regulation of the uptake/release mechanisms involved in ECC in skeletal muscle. If SERCA content were higher in the muscle of dystrophic animals, there would be more protein available to pump Ca^{2+} into the SR and Ca^{2+} uptake rates would likely be higher. Increases in total SERCA content (by increased expression) could be indicative of some compensation that is initiated in response to elevated myoplasmic Ca^{2+} levels. If a protein like PARV were present in higher amounts in mdx/utrn$^{-/-}$ mice, Ca^{2+} would likely be transported and taken up faster than in an animal where PARV levels are reduced. If CSQ levels were lower in dystrophic muscle, Ca^{2+} would not be as effectively sequestered in the SR. Finally, increases in RyR content could lead to more Ca^{2+} being released into the myoplasm of a cell. Surprisingly, no changes were observed in the content of any of these proteins among the three mouse genotypes. There were changes between ages, but these can be accounted for by normal animal development. As the animals grow and age, more protein will be expressed to meet the animals' physiologic needs.

The SR data suggested that faster uptake rates in mdx/utrn$^{-/-}$ mice were not due to changes in SERCA isoform content or total SERCA content. At present, no data has been published about the mdx/utrn$^{-/-}$ mice to support or contradict these observations. With no changes in SERCA content, or in the content of the other Ca^{2+} handling proteins, these data suggest that during development in the dystrophic process, some unidentified regulatory mechanism may be altered that yields increased Ca^{2+} pump activity. For example, this could be an adaptive response to increased $[Ca^{2+}]_i$ to maintain cytosolic Ca^{2+} homeostasis, although at present, there are no available data to support this possibility. If true, however, this would suggest that the increased SERCA activity was a secondary response to the increased $[Ca^{2+}]_i$. This possibility strongly suggests that a time course of $[Ca^{2+}]_i$ in intact dystrophic fibers from mdx:utrn$^{-/-}$ animals aged 9 to 21 days should be assessed, to determine if and when $[Ca^{2+}]_i$ is increased and if the change is paralleled by an increase in SERCA activity. Furthermore, these conclusions should be carefully considered, as they are very much dependent on the assumption that Ca^{2+} is elevated in the myoplasm of mdx and mdx:utrn$^{-/-}$ muscle during maturation, and several studies investigating $[Ca^{2+}]_i$ in dystrophic animals during maturation have revealed no significant differences from control mice. McArdle et al. (1994) demonstrated no significant elevations in $[Ca^{2+}]_i$ in the myoplasm of mdx mouse muscle fibers before the onset of dystrophic changes at 14 days. Furthermore, Collet et al., (1999) observed no differences in $[Ca^{2+}]_i$ in mdx mouse muscle fibers from mice at the

same age. There have been no studies, to date, that have investigated myoplasmic Ca^{2+} concentrations in maturing mdx:utrn$^{-/-}$ mice.

Potential regulators of SR Ca^{2+} uptake and release. Sarcolipin (SLN) regulates SERCA activity in skeletal muscle (MacLennan 2000). Sarcolipin decreases SERCA's affinity for Ca^{2+} at low intracellular Ca^{2+} concentrations. At elevated or saturating Ca^{2+} concentrations, SLN stimulates SERCA Ca^{2+} uptake (Odermatt et al., 1998). The relative content of SLN was not measured in the animals in the present study, but this should be determined in a subsequent study. If the content of SLN is altered in dystrophic muscles, it could provide insight into the faster Ca^{2+} uptake rates observed in mdx/utrn$^{-/-}$ mice. If the levels of SLN are increased in dystrophic muscle, the stimulation it imparts on SERCA at elevated $[Ca^{2+}]_i$ within the muscles should increase. This may allow for increased Ca^{2+} rates by the SR.

Dystrophin and the DGC have been identified as having both structural and intracellular signaling roles (Bredt 1999). The DGC could regulate signal transduction cascades at the sarcolemma via nitric oxide (NO), the product of the nNOS enzyme that associates with the DGC. This potent vasodilator has also been identified as a potential signaling molecule that can affect RyR function and Ca^{2+} ATPase activity (Heunks et al., 2001; Ishii et al., 1998). Heunks et al. (2001) used intact skeletal muscle cells to investigate the effects of NO on SR Ca^{2+} release by assessing $[Ca^{2+}]_i$ in intact myotubes using real-time confocal imaging. In addition to activating release from RyR with acetylcholine and caffeine, myotubes were exposed to different NO donors at varying

concentrations. It was hypothesized that NO would reduce $[Ca^{2+}]_i$ in activated myotubes by oxidation of thiols associated with RyR. The results of the study indicated that NO reduced Ca^{2+} release from the SR of skeletal myotubes. It was apparent that modification of hyper-reactive thiols located on the RyR was responsible for the observed NO-mediated attenuated release (Heunks et al., 2001). nNOS is absent from the sarcolemma of dystrophic muscle (Chang et al., 1996); therefore, intracellular NO levels would likely be reduced. If the inhibition imparted by this molecule is also reduced, Ca^{2+} release may increase in dystrophin deficient fibers, ultimately leading to elevations in $[Ca^{2+}]_i$.

Ishii et al. (1998) demonstrated NO-dependent inhibition of SERCA. Both SERCA activity and Ca^{2+} uptake were inhibited by pretreatment of SR preparations with NO. Because nNOS is absent from muscle sarcolemma in dystrophic muscle, endogenous NO could be decreased in these cells; therefore, the inhibition provided by this component of SERCA regulation could be decreased. This could allow SR Ca^{2+} uptake rates to increase. Perhaps perturbations in NO signaling or another unidentified signaling cascade resulting from the loss of dystrophin, allow for the activity of the Ca^{2+} pump to increase.

Limitations in comparing current investigation with literature. It is difficult to make direct comparisons between this investigation and previously published data. Studies in the available literature used only mdx mice. As yet, the kinetics of Ca^{2+} handling have not been measured in the mdx/utrn$^{-/-}$ mouse at any age. This mouse appears to be a more representative model for the dystrophic disease process (Grady et al., 1997) than the mdx mouse; therefore,

any data obtained from these animals may, in fact, be more indicative of the changes that occur during the dystrophic process. The increased Ca^{2+} uptake observed in mdx:utrn$^{-/-}$ mice may be more closely represent the secondary changes that occur in the onset of DMD in humans.

The majority of studies involving Ca^{2+} kinetics in the muscular dystrophy used older mice (aged 6 weeks or older). These mice can be used to study the physiology of the dystrophic process after onset; however, if the initiation of the disease is of primary interest, the animals must be studied at a much younger age. Results obtained with younger animals may provide better insight into the initiation of the disease process. Increased Ca^{2+} uptake observed in young mdx/utrn$^{-/-}$ mice may be more representative of those secondary changes that occur in the onset of DMD during maturation.

It should also be noted that many of the investigations in which slower uptake values were observed used different methods to obtain their results. In many cases, potent Ca^{2+} chelators (i.e., potassium oxalate) were used for the purposes of initiating uptake into the SR. These methods make it almost impossible to obtain measurable Ca^{2+} release from the SR. Because studying Ca^{2+} release from the SR was a specific aim of this investigation, the aforementioned methods could not be employed. Rather than measuring total calcium uptake into the SR, net Ca^{2+} uptake and release kinetics were measured. It is difficult to make direct comparisons with the data when these two different methods are used; therefore, the same method must be employed to investigate differences between all three genotypes.

Summary. The purpose of this study was to determine how Ca^{2+} homeostasis might be altered in the early stages of DMD, which may account for the onset of disease pathogenesis. Calcium uptake rates observed in the mdx:utrn$^{-/-}$ mouse model of DMD were elevated above those seen in age-matched control and mdx mice. These results differ from the literature, where slowed Ca^{2+} kinetics were observed in older mdx mice. Slowed Ca^{2+} uptake by the SR is a possible cause for elevated myoplasmic Ca^{2+} levels; however, the faster uptake rates observed in maturing mdx/utrn$^{-/-}$ mice suggest the opposite, possibly as an adaptive response to maintain Ca^{2+} homeostasis. Because no differences were observed in the content of Ca^{2+} handling proteins or total SERCA, it is unlikely that protein expression changes, or that alterations in the amount of protein in the muscle accounts for the changes seen in Ca^{2+} cycling by the SR or $[Ca^{2+}]_i$. Instead, there may have been changes in how SERCA was regulated in the dystrophic mouse skeletal muscle that could explain the major findings of this study. Because there are factors involved in Ca^{2+} handling by the SR that were not addressed in this study, it is clear that additional studies are necessary to determine why Ca^{2+} uptake rates are altered in maturing dystrophic mice. Furthermore, it is necessary to investigate other potential mechanisms that yield elevated myoplasmic Ca^{2+} in dystrophic muscles.

Rejection/Non-Rejection of Research Hypotheses. The null hypothesis H_{01} was rejected in the 9-10-day-old mice, as there were differences in the Ca^{2+} uptake rates of mdx and mdx:utrn$^{-/-}$ mice from age-matched control mice ($p > 0.05$). Furthermore, the null hypothesis H_{01} was rejected at 21 days, as mdx:utrn^{-}

$^{-/-}$ mice had significantly higher uptake rates than control and mdx ($p \geq 0.05$). The null hypothesis H_{02} was not rejected for either age group, as there was no effect of age, genotype, or their interaction on release rates for mdx and mdx:utrn$^{-/-}$ mice from control rates observed ($p \geq 0.05$). Finally, null hypotheses H_{03}, H_{04}, H_{05}, H_{06}, H_{07}, and H_{08} were not rejected for both the 9-10 day and 21-day-old sample groups, as there was no effect of age, genotype, or their interaction on content of SERCA, SERCA1, SERCA2, CSQ, PARV, or RyR1 in mdx and mdx:utrn$^{-/-}$ groups compared to control ($p \geq 0.05$).

Future directions. Current literature suggests that elevations in myoplasmic Ca^{2+} in dystrophic muscle fibers may be a cause for the initiation of DMD during maturation. This investigation suggested that Ca^{2+} cycling in general was not compromised, and if anything may have been more effective in mdx:utrn$^{-/-}$ muscles at age 21 days, as SR Ca^{2+} uptake rates were increased. Because total SERCA content and the content of the other Ca^{2+} handling proteins were not altered in the dystrophic muscles, it is logical to suggest that other regulatory mechanisms affecting SERCA may have been modified in the mdx/utrn$^{-/-}$ mice. The content of SLN should be measured in the maturing mice, as this protein could play an essential role in the regulation of Ca^{2+} uptake. To rule out any problems with the Ca^{2+}-ATPases themselves, ATPase activity in the samples should be measured.

Based on the present data, it is not possible to determine if $[Ca^{2+}]_i$ was elevated above normal levels in the dystrophic muscles. Future studies should attempt to measure the levels of myoplasmic Ca^{2+} in mdx/utrn$^{-/-}$ intact muscle

fibers both during maturation (e.g., 9 to 21 days) and following the overt onset of the dystrophic process. As stated earlier, a time course of $[Ca^{2+}]_i$ in intact dystrophic fibers from mdx:utrn$^{-/-}$ animals aged 9 to 21 days, and possibly beyond, should be assessed to determine if and when $[Ca^{2+}]_i$ is increased and if the change is paralleled by an increase in SERCA activity. Finally, it is not likely that alterations in Ca^{2+} uptake by the SR are the primary cause for any elevations in $[Ca^{2+}]_i$. If Ca^{2+} is truly elevated in the myoplasm of mdx:utrn$^{-/-}$ mice during maturation, other sources of Ca^{2+} entry into muscle cells (e.g. Ca^{2+} leak channels in the sarcolemma, DHPR, etc.) or changes in Ca^{2+} homeostasis (e.g. Ca^{2+} uptake by mitochondria) should be investigated in the mdx:utrn$^{-/-}$ mice.

References

1. Adams, B.A., Beam, K.G. (1990). Muscular dysgenesis in mice: a model system for studying excitation-contraction coupling. *FASEB J* 4:2809-2816.
2. Alderton, J.M., Steinhardt, R.A. (2000). How calcium influx through calcium leak channels is responsible for the elevated levels of calcium-dependent proteolysis in dystrophic myotubes. *Trends Cardiovasc Med* 10:268-272.
3. Allamand, V., Campbell, K.P. (2000). Animal models for muscular dystrophy: valuable tools for the development of therapies. *Hum Mol Genet* 9(16):2459-2467.
4. Barriciro, G., Guimaraes, C.R.W., Alencastro, R.B. (2002). A molecular dynamics study of an L-type calcium channel model. *Prot Eng*15(2):109-122.
5. Bean, B.P. (1989). Classes of calcium channels in vertebrate cells. *Annu Rev Physiol* 51:367-384.
6. Berchtold, M.W. (1989). Structure and expression of genes encoding the three-domain Ca2+-binding proteins parvalbumin and oncomodulin. *Biochim Biophys Acta* 1009:201-215.
7. Berchtold, M.W., Brinkmeier, H., Muntener, M. (2000). Calcium ion in skeletal muscle: its crucial role for muscle function, plasticity, and disease. *Phys Rev* 80(3):1215-1265.
8. Bernardi, P. (1999). Mitochondria in muscle cell death. *Ital J Neurol Sci*

20:395-400.

9. Bertorinin, T.E., Bhattacharya, S.K., Palmieri, G.M.A., Chesney, C.M., Pifer, D., Baker, B. (1982). Muscle calcium and magnesium content in Duchenne muscular dystrophy. *Neurol* 32:1088-1092.
10. Bredt, D.S. (1999). Knocking signaling out of the dystrophin complex. *Nat Cell Biol* 1:E89-E91.
11. Brooks, S.V. (1998). Rapid recovery following contraction-induced injury to in situ skeletal muscles in mdx mice. *J Muscle Res Cell Motil* 19:179-187.
12. Bulfield, G., Siller, W.G., Wight, P.A., Moore, K.J. (1984). X chromosome-linked muscular dystrophy (mdx) in the mouse. *Proc. Natl. Acad. Sci. USA* 81:1189-1192.
13. Burkin, D.J., Wallace, G.Q., Nicol, K.J., Kaufman, D.J., Kaufman, S.J. (2001). Enhanced expression of the $\alpha 7\beta 1$ integrin reduces muscular dystrophy and restores viability to dystrophic mice. *J Cell Biol* 152(6):1201-1218.
14. Butcher, L.A., Tomkins, J.K. (1986). Protein profiles of sarcoplasmic reticulum from normal and dystrophic mouse muscle. *J Neurol Sci* 72:159-169.
15. Campbell, K.P. (1995) Three muscular dystrophies: loss of cytoskeleton-extracellular matrix linkage. *Cell* 80:675-679.
16. Carnwath, J.W., Shotton, D.M. (1987). Muscular dystrophy in the mdx mouse: histopathology of the soleus and extensor digitorum longus muscles. *J Neurol Sci* 80:39-54.

17. Chang, W-J., Iannacone, S.T., Lau, K.S., Masters, B.S.S., McCabe, T.J., McMillan, K., Padre, R.C., Spencer, M.J., Tidball, J.G., Stull, J.T. (1996). Neuronal nitric oxide synthase and dystrophin-deficient muscular dystrophy. *Proc. Natl. Acad. Sci.* 93:9142-9147.
18. Collet, C., Allard, B., Tourneur, Y., Jacquemond, V. (1999). Intracellular calcium signals measured with indo-1 in isolated skeletal muscle fibers from control and mdx mice. *J Physiol* 520:417-429.
19. Crosbie, R.H. (2001). NO vascular control in Duchenne muscular dystrophy. *Nat Med* 7(1):27-29.
20. Culligan, K., Banville, N., Dowling, P., Ohlendieck, K. (2002). Drastic reduction of calsequestrin-like proteins and impaired calcium binding in dystrophic mdx muscle. *J Appl Physiol* 92:35-445.
21. Danowski, B.A., Imanaka-Yoshida, K., Sanger, J.M., Sanger, J.W. (1992). Costameres are sites of force transmission to the substratum in adult rat cardiomyoctes. *J Cell Biol* 118(6):1411-20.
22. De Luca, A., Pierno, S., Liantonio, A., Centrone, M., Camerino, C., Simonetti, S., Papadia, F., Camerino, D.C. (2001). Alteration of excitation-contraction coupling mechanism in extensor digitorum longus muscle fibers of dystrophic mdx mouse and potential efficacy of taurine. *Brit J Pharm* 132:1047-1054.
23. Deconinck, A.E., Rafael, J.A., Skinner, J.A., Brown, S.C., Potter, A.C., Metzinger, L., Watt, D.J., Dickson, J.G., Tinsley, J.M., Davies, K.E. (1997). Utrophin-dystrophin-deficient mice as a model for Duchenne muscular

dystrophy. *Cell* 90:717-727.

24. Deconinck, N., Rafael, J.A., Beckers-Bleukx, G. Kahn, D., Deconinck, A.E., Davies, K.E., Gillis, J.M. (1998). Consequences of the combined deficiency in dystrophin and utrophin on the mechanical properties and myosin composition of some limb and respiratory muscles of the mouse. *Neuromusul Disord* 8:362-370.
25. Dettbarn, C., Palade, P. (1998). Effects of three sarcoplasmic/endoplasmic reticulum Ca2+ pump inhibitors on release channels of intracellular stores. *J Pharm Exp Ther* 285(2):739-745.
26. Emery, A.E.H. (1993). Duchenne Muscular Dystrophy, 2nd Ed. (Oxford: Oxford University Press).
27. Felder, E., Protasi, F., Hirsch, R., Franzini-Armstrong, C., Allen, P.D. (2002). Morphology and molecular composition of sarcoplasmic reticulum surface junctions in the absence of DHPR and RyR in mouse skeletal muscle. *Biophys J* 82:3144-3149.
28. Fleischer, S., Inui, M. (1989). Biochemistry and biophysics of excitation-contraction coupling. *Annu Rev Biophys Biophys Che*m 18:333-364.
29. Fong, P., Turner, P.R., Denetclaw, W.F., Steinhardt, R.A. (1990). Increased activity of calcium leak channels in myotubes of Duchenne human and mdx mouse origin. *Science* 250:673-676.
30. Franco, A., Lansman, J.B. (1990). Calcium entry through stretch-inactivated ion channels in mdx myotubes. *Nature* 344:670-673.
31. Gillis, J.M. (1996). Membrane abnormalities and Ca homeostasis in

muscle of the mdx mouse, an animal model of the Duchenne muscular dystrophy: a review. *Acta Physiol Scand* 156:397-406.

32. Grady, R.M., Merlie, J.P., Sanes, J.R. (1997a). Subtle neuromuscular defects in utrophin-deficient mice. *J Cell Biol* 136:871-882.
33. Grady, R.M., Teng, H., Nichol, M.C., Cunningham, J.C., Wilkinson, R.S., Sanes, J.R. (1997). Skeletal and cardiac myopathies in mice lacking utrophin and dystrophin: a model for Duchenne muscular dystrophy. *Cell* 90:729-738.
34. Hoffman, E.P., Brown, R.H.J., Kunkel, L.M. (1987). Dystrophin: The protein product of the Duchenne muscular dystrophy locus. *Cell* 51:919-928.
35. Hollingworth, S., Marshall, M.W., Robson, E. (1990). Excitation contraction coupling in normal and mdx mice. *Muscle Nerve* 13:16-20.
36. Hopf, F.W., Turner, P.R., Denetclaw, W.F., Reddy, P., Steinhardt, R.A. (1996). A critical evaluation of resting intracellular free calcium regulation in dystrophic mdx muscle. *Am J Physiol* 271:C1325-C1339.
37. Hopf, F.W., Reddy, P., Hong, J., Steinhardt, R.A. (1996). A capacitative calcium current in cultured skeletal muscle cells is mediated by the calcium-specific leak channel and inhibited by dihydropyridine compounds. *J Biol Chem* 271(37):22358-22367.
38. Hosfield, C.M., Moldoveanu, T., Davies, P.L., Elce, J.S., Jia, Z. (2001). Calpain mutants with increased Ca^{2+} sensitivity and implications for the role of the C_2-like domain. *J Biol Chem* 276(10):7404-7407.

39. Heunks, L.M.A., Machiels, H.A., Dekhuijzen, P.N.R., Prakash, Y.S., Sieck, G.C. (2001). Nitric oxide affects sarcoplasmic calcium release in skeletal myotubes. *J Appl Physiol* 91:2117-2124.

40. Huxtable, R., Bressler, R. (1973). Effect of taurine on a muscle intracellular membrane. *Biochim Biophys Acta* 323:573-578.

41. Ibraghimov-Beskrovnaya, O., Ervasti, J.M., Leveille, C.J., Slaughter, C.A., Sernett, S.W., Campbell, K.P. (1992) Primary structure of dystrophin-associated glycoproteins linking dystrophin to the extracellular matrix. *Nature* 355:696-702.

42. Kargacin, M.E., Kargacin, G.J. (1996). The sarcoplasmic reticulum calcium pump is functionally altered in dystrophic muscle. *Biochimica et Biophysica Acta* 1290:4-8.

43. Khammari, A., Pereon, Y., Baudet, S., Noireaud, J. (1998). In situ study of the sarcoplasmic reticulum function in control and mdx mouse diaphragm muscle. *Can J Physiol Pharmacol* 76:1161-1165.

44. Klinger, M., Freissmuth, M., Nickel, P., Stabler-Schwarzbart, M., Kassack, M., Suko, J., Hohenegger, M. (1999). Suramin and suramin analogs activate skeletal muscle ryanodine receptor via a calmodulin-binding site. *Mol Pharmacol* 55:462-472.

45. Leberer, E., Hartner, K.T., Pette, D. (1988). Postnatal development of Ca^{2+}-sequestration by the sarcoplasmic reticulum of fast and slow muscles in normal and dystrophic mice. *Eur J Biochem* 174:247-253.

46. Love, D.R., Byth, B.C., Tinsley, J.M., Blake, D.J., Davies, K.E. (1993).

Dystrophin and dystrophin-related proteins: a review of protein and RNA studies. *Neuromuscul Disord* 3(1):5-21.

47. Lunde, P.K., Dahlstedt, A.J., Bruton, J.D., Lannergren, J., Thoren, P., Sejersted, O.M., Westerblad, H. (2001). Contraction and intracellular Ca^{2+} handling in isolated skeletal muscle of rats with congestive heart failure. *Circ Res* 88:1299-1305.
48. Lynch, G.S., Rafael, J.A., Chamberlain, J.S., Faulkner, J.A. (2000). Contraction-induced injury to single permeabilized muscle fibers from mdx, transgenic mdx, and control mice. *Am J Physiol Cell Physiol* 279:C1290-C1294.
49. McArdle, A., Edwards, R.H.T., Jackson, M.J. (1994). Time course of changes in plasma membrane permeability in the dystrophin-deficient mdx mouse. *Muscle Nerve* 17:1378-1384.
50. MacLennan, D.H. (2000). Ca2+ signaling and muscle disease. *Eur J Biochem* 267:5291-5297.
51. Malouk, N., Jacquemond, V., Allard, B. (2000). Elevated subsarcolemmal Ca^{2+} in mdx mouse skeletal muscle fibers detected with Ca^{2+}-activated K+ channels. *PNAS* 97(9):4950-4955.
52. Manttari, S., Pyornila, A., Harjula, R., Jarvilehto, M. (2001). Expression of L-type calcium channels associated with postnatal development of skeletal muscle function in mouse. *J Muscle Res and Cell Mot* 22:61-67.
53. McCarter, G.C., Steinhardt, R.A. (2000). Increased activity of calcium leak channels caused by proteolysis near sarcolemmal ruptures. *J Membrane*

*Bi*ol 176:169-174.

54. McGeachie, J.K., Grounds, M.D. (1999). The timing between skeletal muscle myoblast replication and fusion into myotubes, and the stability of regenerated dystrophic myofibres: an autoradiographic study in mdx mice. *J. Anat.* 194:287-295.
55. Mendell, J.R., Sahenk, Z., Prior, T.W. (1995). The childhood muscular dystrophies: diseases sharing a common pathogenesis of membrane instability. *J Child Neurol* 10:150-159.
56. Melzer, W., Rios, E., Scheider, M.F. (1984). Time course of calcium release and removal in skeletal muscle fibers. *Biophys J* 45:637-641.
57. Moss, R.L. (1992). Ca^{2+} regulation of mechanical properties of striated muscle. *Circ Res* 70(5):865-884.
58. Mukherjee, R., Spinale, F.G. (1998). L-type calcium channel abundance and function with cardiac hypertrophy and failure: a review. *J Mol Cell Cardiol* 30:1899-1916.
59. Nicolas-Metral, V., Raddatz, E., Kucera, P., Ruegg, U.T. (2001). Mdx myotubes have normal excitability but show reduced contraction-relaxation dynamics. *J Muscle Res and Cell Mot* 22:69-75.
60. Odermatt, A., Becker, S., Khanna, V.K., Kurzydlowski, K., Leisner, E., Pette, D., MacLennan, D.H. (1998). Sarcolipin regulates the activity of SERCA1, the fast-twitch skeletal muscle sarcoplasmic reticulum Ca2+-ATPase. *J Biol Chem* 273(20):12360-12369.
61. Ozawa, E., Yoshida, M., Suzuki, A., Mizuno, Y., Hagiwara, Y., Noguchi, S.

(1995). Dystrophin-associated proteins in muscular dystrophy. *Human Mol Genet* 4:1711-1716.

62. Palade, P., Vergara, J. (1982). Arsenazo III and Antipyrylazo III calcium transients in single skeletal muscle fibers. *J Gen Physiol* 79:679-707.
63. Palade, P., Dettbarn, C., Volpe, P., Alderson, B., Otero, A.S. (1989). Direct inhibition of inositol-1,4,5-triphosphate-induced Ca^{2+} release from brain microsomes by K^+ channel blockers. *Molec Pharmacol* 36:664-672.
64. Pasternak, C., Wong, S., Elson, E.L. (1995). Mechanical function of dystrophin in muscle cells. *J Cell Biol* 128(3):355-361.
65. Pereon, Y., Dettbarn, C., Navarro, J., Noireaud, J., Palade, P.T. (1997). Dihydropyridine receptor gene expression in skeletal muscle from mdx and control mice. *Biochimica et Biophysica Acta* 1362:201-207.
66. Petrof, B.J., Shrager, J.B., Stedman, H.H., Kelly, A.M., Sweeney, H.L. (1993) Dystrophin protects the sarcolemmal from stresses developed during muscle contraction. *Proc. Natl. Acad. Sci. USA* 90:3710-3714.
67. Petrof B.J. (1998). The molecular basis of activity-induced muscle injury in Duchenne muscular dystrophy. *Mol and Cellular Biochem* 179:111-123.
68. Pulido, S.M., Passaquin, A.C., Leijendekker, W.J., Challet, C., Wallimann, T., Ruegg, U.T. (1998). Creatine supplementation improves intracellular Ca^{2+} handling and survival in mdx skeletal muscle cells. *FEBS Letters* 439:357-362.
69. Rafael, J.A., Brown, S.C. (2000). Dystrophin and utrophin: genetic analyses of their role in skeletal muscle. *Microsc Res and Tech* 48:155-

166.

70. Roberts, R.G. (2001). Dystrophin & dystrobrevin: protein family review. *Genome Biology* 2(4):3006.1-3006.7.

71. Rome, L.C., Klimov, A.A., Young, I.S. (1999). A new approach for measuring real-time calcium pumping and SR function in muscle fibers. *The Biological Bulletin* 197(2):227.

72. Ruegg, U.T., Gillis, J.M. (1999). Calcium homeostasis in dystrophic muscle. *TiPS* 20:351-352.

73. Satoh, H., Sperelakis, N. (1998). Review of some actions of taurine on ion channels of cardiac muscle cells and others. *Gen Pharmac* 30(4):451-463.

74. Schwaller, B., Dick, J., Dhoot, G., Caroll, s., Vrbova, G., Nicotera, P., Pette, D., Wyss, A., Bluethmann, H., Hunziker, W., Celio, M.R. (1999). Prolonged contraction-relaxation cycle of fast-twitch muscles in parvalbumin knockout mice. *Am J Physiol Cell Physiol* 276:C395-C403.

75. Sicinski, P., Geng, Y., Ryder, C.A., Barnard, E.A., Darlison, M.G., Barnard, P.J. (1989). The molecular basis of muscular dystrophy in the mdx mouse: a point mutation. *Science* 244:1578-1580.

76. Silva, A.C.R., Reinach, F.C. (1991). Calcium binding induces conformational changes in muscle regulatory proteins. *TIBS* 16:53-57.

77. Spencer, M.J., Croall, D.E., Tidball, J.G. (1995). Calpains are activated in necrotic fibers from mdx dystrophic mice. *J Biol Chem* 270:10909-10914.

78. Spencer, M.J., Tidball, J.G. (1996). Calpain translocation during muscle fiber necrosis and regeneration in dystrophin-deficient mice. *Exp Cell Res*

226:264-272.

79. Stedman, H.H., Sweeney, H.L., Shrager, J.B., Maguire, H.C., Panettieri, R.A., Petrof, B., Narusawa, M., Leferovich, J.M., Sladky, J.T., Kelly, A.M. (1991). The mdx mouse diaphragm reproduces the degenerative changes of Duchenne muscular dystrophy. *Nature* 352:536-538.
80. Straub, V., Campbell, K.P. (1997). Muscular dystrophies and the dystrophin-glycoprotein complex. *Current Opinion in Neurology* 10:168-175.
81. Strube, C., Tourneur, Y., Ojeda, C. (2000). Functional expression of the L-type calcium channel in mice skeletal muscle during prenatal myogenesis. *Biophysical Journal* 78:1282-1292.
82. Takagi, A., Kojima, S., Ida, M., Araki, M. (1992). Increased leakage of calcium ion from the sarcoplasmic reticulum of the mdx mouse. *J Neurol Sci* 110:160-164.
83. Tatchencko, A.V., Pietu, G., Cros, N., Gannoun-Zaki, L., Auffray, C., Leger, J.J., Dechesne, C.A. (2001) Identification of altered gene expression in skeletal muscles from Duchenne muscular dystrophy patients. *Neuromusc Disord* 11:269-277.
84. Tidball, J.G., Spencer, M.J. (2000). Calpains and muscular dystrophies. *Int J of Biochem Cell Biol* 32:1-5.
85. Turner, P.R., Westwood, T., Regen, C.M., Steinhardt, R.A. (1988). Increased protein degradation results form elevated free calcium levels found in muscle from *mdx* mice. Nature 335:735-738.

86. Turner, P.R., Fong, P., Denetclaw, W.F., Steinhardt, R.A. (1991) Increased calcium influx in dystrophic muscle. *J Cell Biol* 115(6):1701-1712.

87. Vandebrouck, C., Imbert, N., Constantin, B., Duport, G., Raymond, G., Cognard, C. (2002). Normal calcium homeostasis in dystrophin-expressing facioscapulohumeral muscular dystrophy myotubes. *Neuromusc Disord* 12:266-272.

88. Ward, C.W., Spangeburg, E.E., Diss, L.M., Williams, J.W. (1998). Effects of varied fatigue protocols on sarcoplasmic reticulum calcium uptake and release rates. *Am J Physio*l 275:R1-R6.

89. Wehling, M., Spencer, M.J., Tidball, J.G. (2001). A nitric oxide synthase transgene ameliorates muscular dystrophy in mdx mice. *J Cell Biol* 155:123-131.

90. Worton, R. (1995). Muscular dystrophies: diseases of the dystrophin-glycoprotein complex. *Science* 270:755-756.

Appendix A: Summary of DMD literature with respect to calcium handling in dystrophic muscle.

Author & Pub. Year	Mouse Model	Age of Animals used	Aspect of Ca^{2+} handling addressed	Major Findings
Turner et al., 1988	Mdx	"Adult"	$[Ca^{2+}]_i$ at rest and during stimulation	(1) Marked elevations at rest and during stimulation in mdx mice from control; (2) Slowed transient kinetics in mdx mice.
Fong et al., 1990	Mdx myotubes	6-15 days after fusion	$[Ca^{2+}]_i$ at rest with various extracellular Ca^{2+} concentrations	(1) Increase in the activity of Ca^{2+} leak channels in dystrophic myotubes contributed to elevations in $[Ca^{2+}]_i$
Turner et al., 1991	Mdx myotubes	Mice 3-6 wks; myotubes 2 days after differentiation	$[Ca^{2+}]_i$ at rest & leak channel activity	(1) $[Ca^{2+}]_i \uparrow$ in the dystrophic myotubes; (2) Leak through DHPR not contributing; (3) Ca^{2+} leaking into myotubes through leak channels; (4) Slowed transient kinetics in mdx myotubes
Nicolas-metral et al., 2001	Mdx myotubes	Mice 1-3 days; myotubes 2-3 weeks after fusion	Cellular excitability, contraction, & relaxation	(1) A slowed contraction-relaxation process in dystrophic myotubes was evidence of a dysregulation in Ca^{2+} homeostasis.
Grange et al., 2002	Mdx	9-12 days	Contraction/ Relaxation of whole EDL muscles	(1) Slowed contraction relaxation dynamics in mdx, and mdx:utrn$^{-/-}$ mice.
De Luca et al., 2001	Mdx	8-10 weeks; 6-8 months	Voltage threshold for activation of ECC	(1) The ECC mechanism is altered in dystrophin-deficient mouse muscle at ages $\geq$ 4 months.

Leberer et al., 1988	Mdx	Birth to 36 weeks	Ca^{2+}-uptake activities of the SR	(1) No differences in Ca^{2+} uptake between control and mdx muscle until after 6 weeks-of-age; (2) Slowed Ca^{2+} uptake in dystrophic animals was, very likely, a secondary effect caused by another initial insult in the case of dystrophy
Kargacin et al., 1996	Mdx	8 weeks	Ca^{2+} -uptake activities of the SR	(1) Maximum velocity of uptake was less for the mdx mice.
Takagi et al., 1992	Mdx	4-8 weeks	Contractile regulation & Ca^{2+} cycling by the SR	(1) No differences in uptake rates and rate of CICR; (2) Ca^{2+} leaked at a significantly faster rate in mdx fibers; (3) Increased leakage of Ca^{2+} via the RyR has the potential to contribute to higher $[Ca^{2+}]_i$ in dystrophic muscle fibers.
McArdle et al., 1994	Mdx	14 days; 40 days	$[Ca^{2+}]_i$ in muscle fibers	(1) No difference in $[Ca^{2+}]_i$ in the myoplasm of mdx muscle fibers at 14-days; (2) $\uparrow$ $[Ca^{2+}]_i$ in the myoplasm of mdx muscle fibers at 40-days; (3) Increasing $[Ca^{2+}]_i$ in mdx muscle is secondary to degeneration process occurring in this muscle
Collet et al., 1999	Mdx	~2-50 weeks	$[Ca^{2+}]_i$ in muscle fibers at rest and during depolarization	(1) No significant changes were noted in $[Ca^{2+}]_i$ between control and mdx fibers at rest and during depolarization.
Khammari et al., 1998	Mdx	7-8 weeks	Ca^{2+} -uptake activities of the SR of diaphragm	(1) No significant differences in rate of Ca^{2+} uptake from the myoplasm.
Butcher et al., 1986	Mdx	3 months	Protein content of various Ca^{2+}	(1) Content of SERCA and CSQ was decreased in dystrophic muscles.

			handling proteins	
Pereon et al., 1997	Mdx	9-11 weeks	Gene expression of DHPR	(1) ↑ gene expression of DHPR in dystrophic muscle did not lead to increases in the content of functional DHPR in dystrophic from control muscle
Culligan et al., 2001	Mdx	8 weeks	Protein content of various Ca^{2+} handling proteins	(1) No significant differences in the content of DHPR, SERCA, RyR, and CSQ; (2) drastic declines in the content “calsequestrin-like proteins” in mdx mouse muscle
Badalamente et al., 2000	Mdx	14 days	Calpain activity and muscle fiber degeneration	(1) Calpain contributes to an increased proteolysis in dystrophic muscle; (2) This is a negative effect of elevated $[Ca^{2+}]_i$ on muscle fibers.
Alterton and Steinhardt 2000	Mdx myotubes	???	Calpain activity and muscle fiber degeneration	(1) The accumulated effects of long-term contractile activity and long-term calpain proteolysis give rise to the differences seen in Ca^{2+} homeostasis

Appendix B: Raw Data

Number	Genotype	Age	Muscle wwt (mg)	Uptake Rate	Release Rate
2248a1	CONT	9.000	36.3	0.591	0.228
C57BL6p5	CONT	9.000	29.5	0.373	0.136
2248a2	CONT	9.000	37.0	0.428	0.437
2248a3	CONT	9.000	36.8	0.453	0.158
2246a5	CONT	9.000	30.2	0.581	0.269
2246a2	CONT	9.000	30.0	0.199	0.110
Mean			**33.300**	**0.437**	**0.223**
SEM			**1.526**	**0.059**	**0.049**
2269ap3	DKO	10.000	28.3	0.195	0.186
1781ap4	DKO	10.000	33.5	0.387	0.263
1781ap7	DKO	10.000	32.7	0.428	0.246
2273ap1	DKO	10.000	20.7	0.391	0.167
1781ap1	DKO	10.000	29.8	0.264	0.391
Mean			**29.000**	**0.333**	**0.251**
SEM			**2.280**	**0.044**	**0.039**
2217bp2	mdx	9.000	17.0	0.360	0.121
1864m6	mdx	9.000	54.5	0.738	0.260
1864m5	mdx	9.000	51.9	0.655	0.280
1864m2	mdx	9.000	50.5	0.347	0.434
2217bp3	mdx	9.000	33.4	0.679	0.413
2217bp4	mdx	9.000	31.9	0.893	0.243
Mean			**39.867**	**0.612**	**0.292**
SEM			**6.056**	**0.089**	**0.047**
2248a6	CONT	21.000	130.0	0.644	0.236
2246a11	CONT	21.000	95.4	0.566	0.275
2246a10	CONT	21.000	96.3	0.684	0.205
2246a9	CONT	21.000	91.2	0.978	0.238
2246a8	CONT	21.000	120.0	0.688	0.137
2248a5	CONT	21.000	120.0	0.644	0.236
Mean			**108.817**	**0.701**	**0.221**
SEM			**6.698**	**0.058**	**0.019**
2262ap9	DKO	21.000	89.3	1.380	0.081
2206ap2	DKO	21.000	94.7	1.725	0.235
2262ap6	DKO	21.000	88.5	1.087	0.190
2262ap2	DKO	21.000	119.7	1.531	0.120
2206ap4	DKO	21.000	99.7	1.435	0.392
Mean			**98.380**	**1.432**	**0.204**
SEM			**5.700**	**0.104**	**0.054**
1865dp11	mdx	21.000	105.8	0.546	0.213
1865dp6	mdx	21.000	101.4	0.937	0.110

1865dp10	mdx	21.000	86.2	0.726	0.195
1865dp9	mdx	21.000	111.0	0.881	0.381
1865dp8	mdx	21.000	119.0	0.848	0.183
1865dp7	mdx	21.000	97.1	0.974	0.149
Mean			**103.417**	**0.819**	**0.205**
SEM			**4.642**	**0.065**	**0.038**

Number	Genotype	Age	SERCA 1 content	SERCA 2 content	Total SERCA
2248a1	CONT	9.000	0.169	0.000	0.591
C57BL6p5	CONT	9.000	0.163	0.000	0.402
2248a2	CONT	9.000	0.170	0.000	0.442
2248a3	CONT	9.000	0.200	0.000	0.573
2246a5	CONT	9.000	0.000	0.000	0.591
2246a2	CONT	9.000	0.000	0.000	0.399
Mean			**0.117**	**0.000**	**0.500**
SEM			**0.037**	**0.000**	**0.039**
2269ap3	DKO	10.000	0.000	0.000	0.391
1781ap4	DKO	10.000	0.163	0.000	0.472
1781ap7	DKO	10.000	0.052	0.000	0.528
2273ap1	DKO	10.000	0.000	0.000	0.480
1781ap1	DKO	10.000	0.038	present	0.447
Mean			**0.051**	**20% of samples**	**0.464**
SEM			**0.030**	**0.000**	**0.022**
2217bp2	mdx	9.000	0.264	0.000	0.543
1864m6	mdx	9.000	0.513	0.000	0.667
1864m5	mdx	9.000	0.299	0.000	0.588
1864m2	mdx	9.000	0.000	0.000	0.482
2217bp3	mdx	9.000	0.311	0.000	0.611
2217bp4	mdx	9.000	0.499	present	0.745
Mean			**0.314**	**16.7% of samples**	**0.606**
SEM			**0.076**	**0.000**	**0.038**
2248a6	CONT	21.000	0.758	0.000	0.838
2246a11	CONT	21.000	0.667	present	0.699
2246a10	CONT	21.000	0.691	0.000	0.907
2246a9	CONT	21.000	0.944	present	1.104
2246a8	CONT	21.000	0.431	0.000	0.929
2248a5	CONT	21.000	1.184	present	0.896
Mean			**0.779**	**50% of samples**	**0.896**
SEM			**0.105**	**0.000**	**0.054**

2262ap9	DKO	21.000	1.312	present	0.985
2206ap2	DKO	21.000	0.663	present	1.187
2262ap6	DKO	21.000	1.193	present	0.743
2262ap2	DKO	21.000	1.171	0.000	1.110
2206ap4	DKO	21.000	0.882	present	1.040
Mean			**1.044**	**80%of samples**	**1.013**
SEM			**0.119**	**0.000**	**0.076**

1865dp11	mdx	21.000	0.642	present	0.659
1865dp6	mdx	21.000	0.787	present	0.955
1865dp10	mdx	21.000	0.429	0.000	0.790
1865dp9	mdx	21.000	0.660	0.000	0.990
1865dp8	mdx	21.000	0.880	0.000	0.889
1865dp7	mdx	21.000	1.198	0.000	1.015
Mean			**0.766**	**33% of samples**	**0.883**
SEM			**0.106**	**0.000**	**0.056**

Number	Genotype	Age	PARV content	RyR1	RyR frag	RyR Total	CSQ
2248a1	CONT	9.000	0.605	0.000	1.470	1.470	0.000
C57BL6p5	CONT	9.000	0.671	0.000	0.794	0.794	0.215
2248a2	CONT	9.000	0.808	0.512	0.995	1.506	0.260
2248a3	CONT	9.000	0.712	0.738	0.978	1.716	0.120
2246a5	CONT	9.000	0.453	0.434	0.291	0.725	0.415
2246a2	CONT	9.000	0.492	0.148	0.359	0.507	0.218
Mean			**0.624**	**0.305**	**0.815**	**1.120**	**0.205**
SEM			**0.055**	**0.124**	**0.180**	**0.205**	**0.057**

2269ap3	DKO	10.000	0.593	0.191	0.137	0.328	0.245
1781ap4	DKO	10.000	0.715	0.000	0.956	0.956	0.148
1781ap7	DKO	10.000	0.637	0.000	1.468	1.468	0.165
2273ap1	DKO	10.000	0.322	0.637	0.977	1.614	0.000
1781ap1	DKO	10.000	0.614	0.587	0.295	0.882	0.306
Mean			**0.576**	**0.283**	**0.767**	**1.050**	**0.173**
SEM			**0.067**	**0.139**	**0.244**	**0.229**	**0.052**

2217bp2	mdx	9.000	0.354	0.616	0.880	1.496	0.000
1864m6	mdx	9.000	0.830	0.000	1.004	1.004	0.300
1864m5	mdx	9.000	0.610	0.402	0.223	0.625	0.652
1864m2	mdx	9.000	0.575	0.482	0.640	1.123	0.503
2217bp3	mdx	9.000	0.626	0.499	0.226	0.724	0.358
2217bp4	mdx	9.000	0.651	0.128	0.322	0.449	0.662
Mean			**0.608**	**0.354**	**0.549**	**0.903**	**0.412**
SEM			**0.062**	**0.097**	**0.140**	**0.156**	**0.102**

2248a6	CONT	21.000	0.885	1.102	1.273	2.375	0.765
2246a11	CONT	21.000	1.006	0.997	0.920	1.917	0.747

2246a10	CONT	21.000	1.050	0.378	1.521	1.899	0.547
2246a9	CONT	21.000	1.034	0.603	1.588	2.191	0.527
2246a8	CONT	21.000	0.946	0.000	1.477	1.477	0.715
2248a5	CONT	21.000	0.973	0.000	1.571	1.571	0.501
Mean			**0.982**	**0.513**	**1.392**	**1.905**	**0.634**
SEM			**0.025**	**0.194**	**0.105**	**0.141**	**0.049**

2262ap9	DKO	21.000	0.980	0.416	2.640	3.057	0.907
2206ap2	DKO	21.000	0.846	0.667	1.301	1.968	0.559
2262ap6	DKO	21.000	1.036	0.595	1.340	1.935	0.856
2262ap2	DKO	21.000	0.969	0.729	1.123	1.851	0.514
2206ap4	DKO	21.000	0.769	0.432	1.071	1.503	0.750
Mean			**0.920**	**0.568**	**1.495**	**2.063**	**0.717**
SEM			**0.049**	**0.062**	**0.291**	**0.262**	**0.078**

1865dp11	mdx	21.000	1.001	0.693	1.193	1.886	0.954
1865dp6	mdx	21.000	0.994	0.722	1.026	1.748	0.455
1865dp10	mdx	21.000	0.926	0.000	2.020	2.020	0.394
1865dp9	mdx	21.000	0.947	0.421	1.336	1.757	0.818
1865dp8	mdx	21.000	1.205	0.000	1.646	1.646	0.647
1865dp7	mdx	21.000	1.178	0.656	2.449	3.106	0.710
Mean			**1.042**	**0.415**	**1.612**	**2.027**	**0.663**
SEM			**0.049**	**0.138**	**0.221**	**0.222**	**0.087**

Appendix C: Statistical Analyses

Two Way Analysis of Variance for Uptake Rates					
Source of Variation	**DF**	**SS**	**MS**	**F**	**P**
Genotype	2	0.535	0.268	9.087	<0.001
Age (d)	1	2.306	2.306	78.305	<0.001
Genotype x Age (d)	2	1.321	0.661	22.429	<0.001
Residual	28	0.825	0.0295		
Total	33	4.713	0.143		

Two Way Analysis of Variance for Release Rates					
Source of Variation	**DF**	**SS**	**MS**	**F**	**P**
Genotype	2	0.00466	0.00233	0.299	0.797
Age (d)	1	0.0172	0.0172	1.693	0.204
Genotype x Age (d)	2	0.0108	0.00540	0.532	0.593
Residual	28	0.285	0.0102		
Total	33	0.317	0.00962		

Two Way Analysis of Variance for Total SERCA Content					
Source of Variation	**DF**	**SS**	**MS**	**F**	**P**
Genotype	2	0.0153	0.00765	0.547	0.584
Age (d)	1	1.400	1.400	100.165	<0.001
Genotype x Age (d)	2	0.101	0.0506	3.620	0.040
Residual	28	0.391	0.0140		
Total	33	1.862	0.0564		

Two Way Analysis of Variance for SERCA1 Content					
Source of Variation	**DF**	**SS**	**MS**	**F**	**P**
Genotype	2	0.0709	0.0355	0.834	0.445
Age (d)	1	4.164	4.164	97.982	<0.001
Genotype x Age (d)	2	0.403	0.201	4.742	0.017
Residual	28	1.190	0.0425		
Total	33	5.656	0.171		

Two Way Analysis of Variance for SERCA 2 Content					
Source of Variation	**DF**	**SS**	**MS**	**F**	**P**
Genotype	2	0.441	0.221	1.173	0.324
Age (d)	1	1.504	1.504	7.997	0.009
Genotype x Age (d)	2	0.292	0.146	0.777	0.470
Residual	28	5.267	0.188		
Total	33	7.441	0.225		

Two Way Analysis of Variance for CSQ Content					
Source of Variation	**DF**	**SS**	**MS**	**F**	**P**
Genotype	2	0.0923	0.0461	1.457	0.250
Age (d)	1	1.404	1.404	44.360	<0.001
Genotype x Age (d)	2	0.122	0.0609	1.922	0.165
Residual	28	0.886	0.0317		
Total	33	2.460	0.0745		

Two Way Analysis of Variance for PARV Content					
Source of Variation	**DF**	**SS**	**MS**	**F**	**P**
Genotype	2	0.0334	0.0167	1.073	0.356
Age (d)	1	1.212	1.212	77.959	<0.001
Genotype x Age (d)	2	0.0134	0.00671	0.432	0.654
Residual	28	0.435	0.0155		
Total	33	1.716	0.0520		

Two Way Analysis of Variance for RyR1 Content					
Source of Variation	**DF**	**SS**	**MS**	**F**	**P**
Genotype	2	0.00922	0.00461	0.0443	0.957
Age (d)	1	0.287	0.287	2.760	0.108
Genotype x Age (d)	2	0.0724	0.0362	0.348	0.709
Residual	28	2.915	0.104		
Total	33	3.268	0.0990		

Two Way Analysis of Variance for 410 kDa Frag Content					
Source of Variation	**DF**	**SS**	**MS**	**F**	**P**
Genotype	2	0.0138	0.00692	0.0311	0.969
Age (d)	1	5.257	5.257	23.612	<0.001
Genotype x Age (d)	2	0.368	0.184	0.827	0.448
Residual	28	6.234	0.223		
Total	33	11.961	0.362		

Two Way Analysis of Variance for Total RyR1 Content					
Source of Variation	**DF**	**SS**	**MS**	**F**	**P**
Genotype	2	0.0453	0.0226	0.0977	0.907
Age (d)	1	8.006	8.006	34.532	<0.001
Genotype x Age (d)	2	0.178	0.0889	0.383	0.685
Residual	28	6.491	0.232		
Total	33	14.741	0.447		

Curriculum Vitae

Matthew Robert Rittler was born on July 25, 1978 in Carroll County, Maryland. He graduated from North Carroll High School in Carroll County, Maryland in 1996 and, after that, began his college career at Western Maryland College. He graduated, summa cum laude, in May of 2000 with two Bachelor of Arts degrees in Biochemistry and Exercise-Chemistry, respectively. He spent the next two years at Virginia Polytechnic Institute and State University working towards a Master of Science degree in muscle physiology and biochemistry. After earning his degree, he plans on continuing his education by working to obtain a Ph.D. from the College of Veterinary Medicine at Virginia Polytechnic Institute and State University.